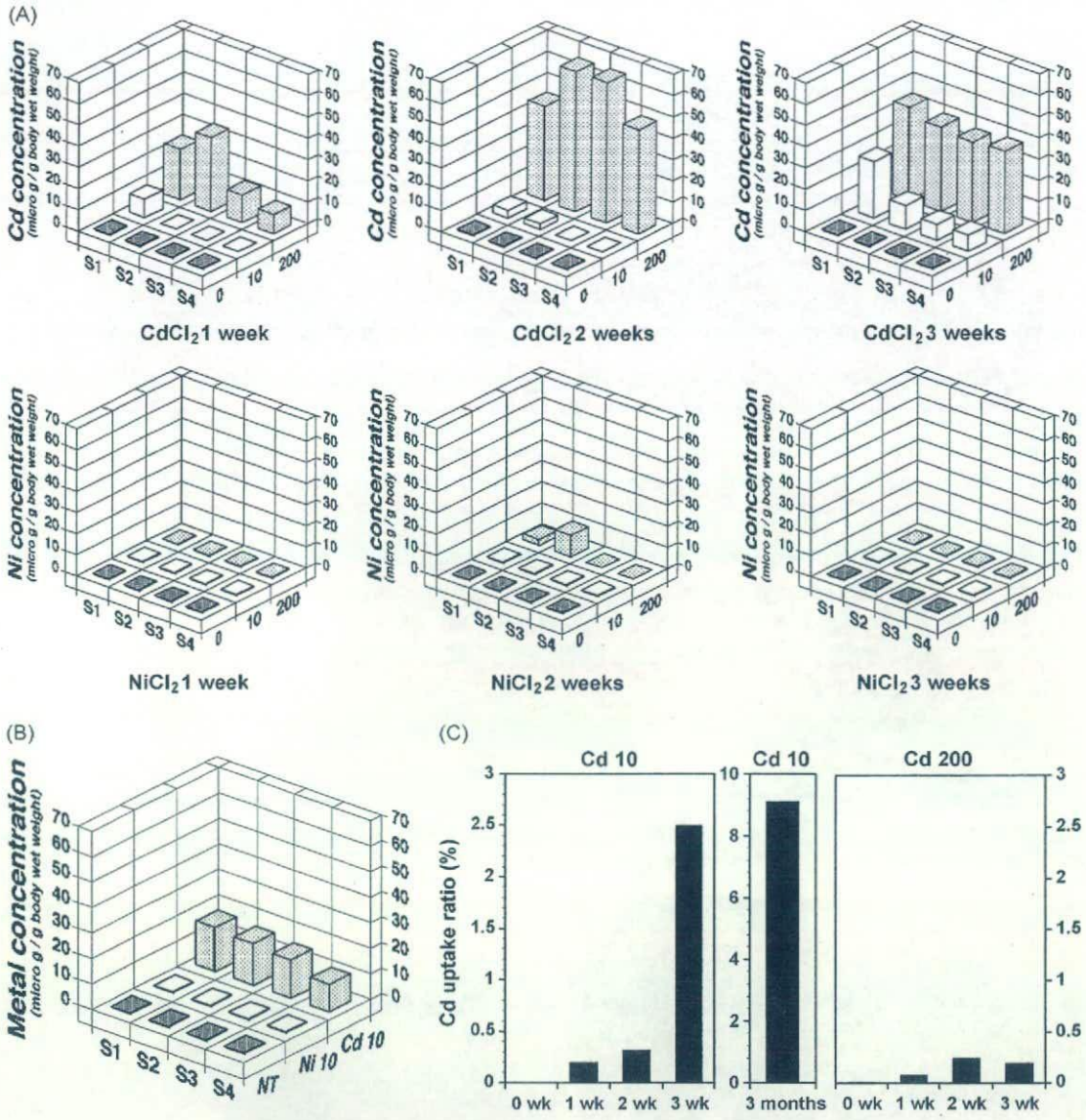

Fig. 3. Heavy metal accumulation in *E. fetida* in the short-term (A) and the long-term (B) experiments. Each data point represents the mean of three individuals. Heavy metal concentrations were measured by atomic absorption spectrometry, and are expressed as micrograms per gram of body wet weight. The percentage ratio of the uptake of Cd within 50 g soil by all *E. fetida* per container was calculated and shown (C).

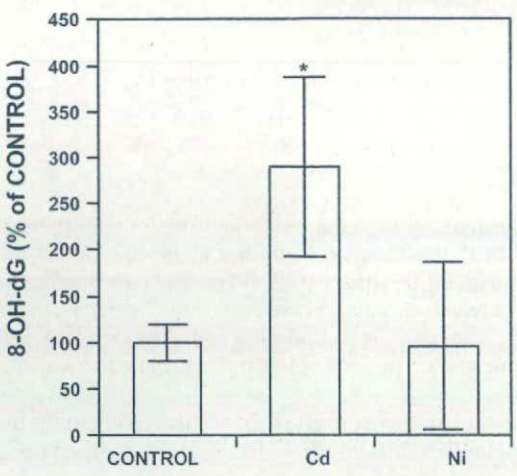

weeks) (Fig. 3A). To the contrary, Ni accumulation was not observed during this experiment, except for one individual data set (200 μg Ni/g soil, 2 weeks). In a long-term experiment, accumulation of Cd, not Ni, was detected in all segments (Fig. 3B). To determine how much the earthworms clean up the soil, the Cd uptake ratio by *E. fetida* was calculated. *E. fetida* took up at most ~2.5% of the Cd in 50 g soil in a short-term experiment and ~9% of the Cd in 50 g soil in a long-term experiment (Fig. 3C).

3.3. Accumulation levels of 8-OH-dG in the earthworm DNA

The 8-OH-dG levels in the DNA of earthworms treated with $CdCl_2$ for 3 months were significantly higher than those in control

Fig. 4. The 8-OH-dG levels in DNA from the S1 region of earthworms (3-month experiment) were analyzed by HPLC equipped with electrochemical detection. The values were expressed as % of control value. Mean values ± S.D., $n = 5$. Significant differences from the control group and Ni-treated group: $^{*}p < 0.005$ *vs.* control group, $p < 0.05$ versus Ni-treated group.

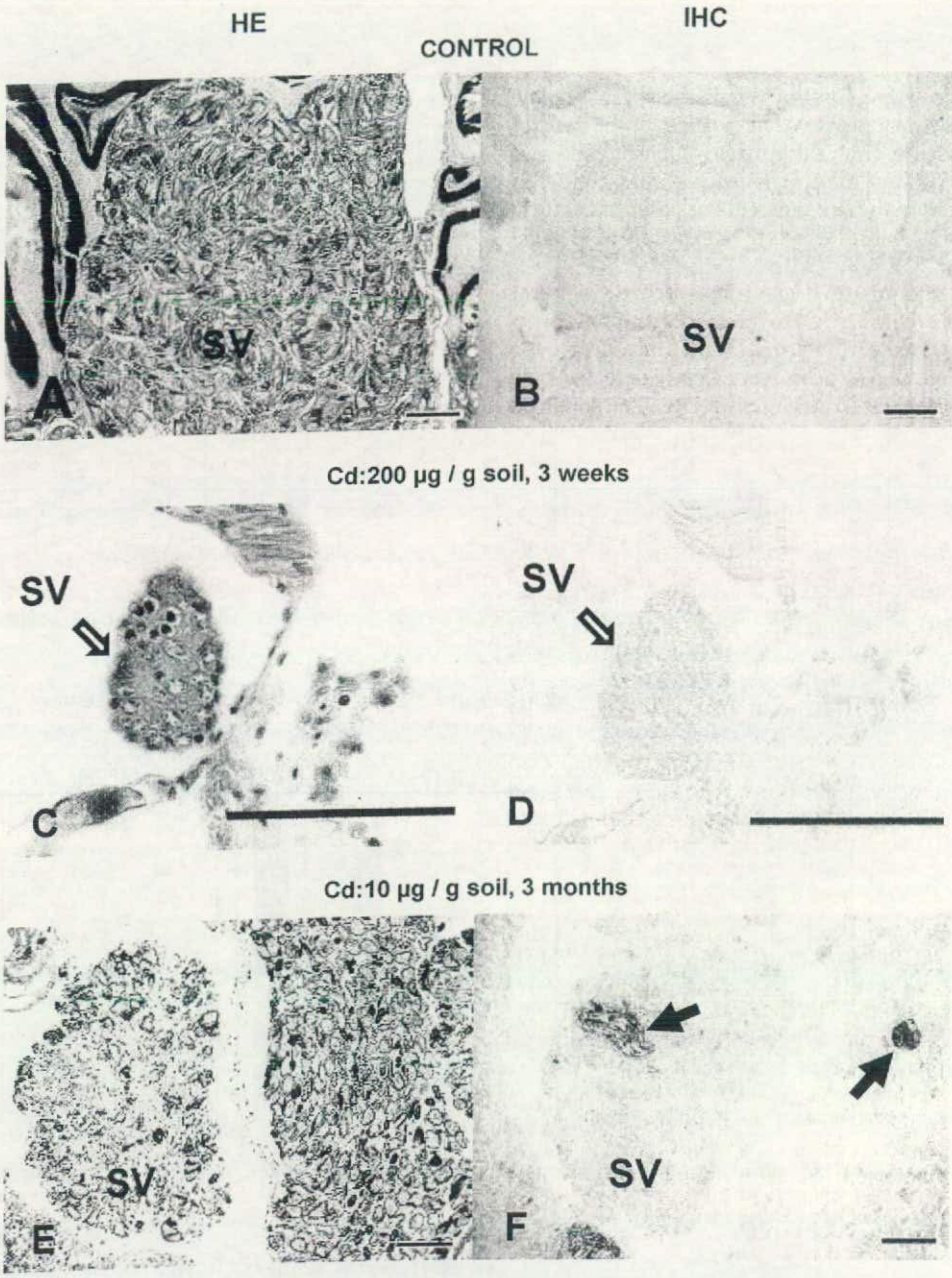

Fig. 5. Immunohistochemical analyses of 8-OH-dG accumulation in the seminal vesicles of *E. fetida* (S1) treated with Cd (200 μg/g soil, 3 weeks; HE (C), IHC (D)), and Cd (10 μg/g soil, 3 months; HE (E), IHC (F)). Controls: (A) and (B). Positive signals for 8-OH-dG accumulation in the seminal vesicles were detected only in *E. fetida* treated with Cd (10 μg/g soil) for 3 months. HE stained section and IHC stained section are in several serial sections. Arrowheads (black) show positive signals in seminal vesicles. SV: seminal vesicles. All scale bars are 100 μm.

earthworms or in earthworms treated with $NiCl_2$ (Fig. 4). These results are compatible with those from the immunohistochemical analyses, in which positive signals for 8-OH-dG in seminal vesicles (in S1 region) were clearly detected.

3.4. Immunohistochemical detection of 8-OH-dG accumulation in *E. fetida*

Positive signals in seminal vesicles were detected only in *E. fetida* treated with 10 μg Cd for 3 months (Fig. 5). Besides these signals, no significant difference was detected in the other metal-treated specimens in comparison to the control. In addition, 8-OH-dG accumulation was detected in the gut epithelial layers in almost all specimens (data not shown). Since ROS are easily generated by non-specific environmental factors, it is reasonable that 8-OH-dG was present in almost all gut epithelial layers.

4. Discussion

Among the many kinds of living organisms in soil, the earthworm is a most useful organism for the evaluation of metal contamination in soil, because significant positive correlations have been found between the metal concentrations in the earthworm and the soil Cd, copper, lead and zinc concentrations [41]. This evidence prompted us to verify the utility of the earthworm as a bio-monitor.

In the present study, we observed Cd accumulation in the anterior segment of the earthworm *E. fetida* at an early stage and

gradually almost equally in all four segments, suggesting that Cd might be accumulated in multiple organs (Fig. 3). It is well known that one biological effect of some heavy metals, such as Cd accumulation, in organisms is growth inhibition [42]. In the present study, the body wet weight of *E. fetida* decreased to 49.5% of the control by 200 μg Cd/g soil exposure. Thus, the growth inhibition observed in the present study indicated that the *E. fetida* actually suffered from the Cd accumulated in their organs. On the other hand, little Ni accumulation and no inhibitory effects of Ni exposure on *E. fetida* growth were observed.

We observed increased 8-OH-dG levels in DNA of the S1 region of Cd-treated earthworms in comparison to the other groups of earthworms (control or Ni-treated earthworms) (Fig. 4). In addition, the positive signals in the seminal vesicles were clearly detected only in *E. fetida* treated with 10 μg of Cd at 3 months (Fig. 5), although Cd accumulation was detected in all S1 segments, including the 200 μg Cd-exposed specimens, in which seminal vesicles were located. These findings seemed to be specific to long-term Cd exposure, and raised the question of why Cd treatment of *E. fetida* increased the 8-OH-dG accumulation only in that organ. One possible explanation for this question is the distribution of metal-binding proteins. On the other hand, we observed positive staining of 8-OH-dG in the gut epithelial layers in almost all samples. The metal absorption routes include the digestive system and the surface wall [43,44], but the main route is the digestive system. Since gut epithelial layers are frequently exposed to ROS, 8-OH-dG accumulation was constantly detected.

In mammals, the cysteine-rich metal-binding protein, metallothionein (MT), exists especially in the liver and kidney, and plays a key role in metal detoxification. However, mammalian testes and ventral prostate had either no induction or a reduced expression of the MT gene when the animals were exposed to Cd or some other MT-inducing agents [45,46]. MT is a ubiquitous metal-binding protein found in plants, invertebrates including earthworm, and mammals. Earthworm MT, which has two isoforms (MT-1 and MT-2), was also identified and cloned [47]. Recently, MT expression was detected in the intestinal region, chlorangogenous tissue, and gut of *Lumbricus rubellus* collected from an arsenic/copper-contaminated site [48]. Thus, MT expression plays a key role in Cd-induced toxicity or mutagenicity.

In the present study, positive signals for 8-OH-dG accumulation were detected in the seminal vesicles, which are considered as MT-poor organs. Therefore, it seems reasonable to speculate that a lower level of MT expression is involved in Cd-induced DNA damage accumulation. To address this speculation, the relationship between the localizations of Cd, MT, and 8-OH-dG accumulation should be clarified as a further study. Moreover, the seminal vesicles are located in S1, in which Cd accumulated from an early stage, suggesting that long-term exposure to Cd might also contribute to an increase in 8-OH-dG accumulation in seminal vesicles. Thus, it is reasonable to conclude that an increase in 8-OH-dG accumulation in seminal vesicles might reflect long-term exposure to Cd.

The carcinogenic potentials of Cd and Ni have been established for humans and experimental animals [32,33]. In addition, both Cd and Ni are known to increase 8-OH-dG generation in human and animal DNA [14,34–36]. Hence, we employed Cd and Ni as test metals. In the present study, we observed a high level of Cd accumulation and little Ni accumulation in *E. fetida*, accompanied with an increase in 8-OH-dG accumulation in the seminal vesicles of Cd-exposed *E. fetida*. Based on these results, it is reasonable to conclude that the increase in 8-OH-dG accumulation is due to Cd accumulation and incomplete metal detoxification in the seminal vesicles of *E. fetida*. In addition, Cd reportedly inhibited 8-OH-dGTPase activity, but Ni did not [31]. This evidence might also explain the differences in the levels of 8-OH-dG accumulation.

Taken together, our results demonstrate the possible utility of a bio-monitoring method for assessing soil mutagenicity, by using earthworms as bio-monitors and measuring the oxidative DNA damage generated in the earthworm. Immunohistochemical analyses are useful to detect the locations of 8-OH-dG accumulation, but unlike HPLC analyses, they are not quantitative. Therefore, a method using both HPLC and immunohistochemical analyses is recommended. However, many points remain unresolved. For example, this method could be reliable only for bio-accumulated metals, such as Cd, but not for non-bio-accumulated metals, such as Ni, even if they generate 8-OH-dG. To establish a bio-monitoring method using earthworms for soil mutagenicity, further studies will be required.

Acknowledgements

We would like to express our thanks to Dr. C.A. Edwards (Ohio State University) for providing the *E. fetida* and Ikesue Toyotada Shoten (Mizuma-gun, Japan) for the supply of scrapped mold. This work was supported by a grant from The Foundation for Earth Environment.

References

[1] M. Vidovic, A. Sadibasic, S. Cupic, M. Lausevic, Cd and Zn in atmospheric deposit, soil, wheat, and milk, Environ. Res. 97 (2005) 26–31.
[2] M. Harnly, S. Seidel, P. Rojas, R. Fornes, P. Flessel, D. Smith, R. Kreutzer, L. Goldman, Biological monitoring for mercury within a community with soil and fish contamination, Environ. Health Perspect. 105 (1997) 424–429.
[3] F. Regoli, S. Gorbi, D. Fattorini, S. Tedesco, A. Notti, N. Machella, R. Bocchetti, M. Benedetti, F. Piva, Use of the land snail *Helix aspersa* as sentinel organism for monitoring ecotoxicologic effects of urban pollution: an integrated approach, Environ. Health Perspect. 114 (2006) 63–69.
[4] S. Citterio, R. Aina, M. Labra, A. Chiani, P. Fumagalli, S. Sgorbati, A. Santagostino, Soil genotoxicity assessment: a new strategy based on biomolecular tools and plant bioindicators, Environ. Sci. Technol. 36 (2002) 2748–2753.
[5] F. Brulle, G. Mitta, C. Coquerelle, D. Vieau, S. Lemiere, A. Leprêtre, F. Vandenbulcke, Cloning and real-time PCR testing of 14 potential biomarkers in *Eisenia fetida* following cadmium exposure, Environ. Sci. Technol. 40 (2006) 2844–2850.
[6] A.J. Reinecke, S.A. Reinecke, Earthworm as test organisms in ecotoxicological assessment of toxicant impacts on ecosystems, in: C.A. Edwards (Ed.), Earthworm Ecology, CRC Press LLC, Boca Baton, FL, 2004, pp. 299–320.
[7] N.T.T.M. Steenbergen, F. Iaccino, M. De Winkel, L. Reijnders, W.J.G.M. Peijnenburg, Development of a biotic ligand model and a regression model predicting acute copper toxicity to the earthworm *Aporrectodea caliginosa*, Environ. Sci. Technol. 39 (2005) 5694–5702.
[8] M.L. Wood, M. Dizdaroglu, E. Gajewski, J.M. Essigmann, Mechanistic studies of ionizing radiation and oxidative mutagenesis: genetic effects of a single 8-hydroxyguanine (7-hydro-8-oxoguanine) residue inserted at a unique site in a viral genome, Biochemistry 29 (1990) 7024–7032.
[9] S. Shibutani, M. Takeshita, A.P. Grollman, Insertion of specific bases during DNA synthesis past the oxidation-damaged base 8-OH-dG, Nature 349 (1991) 431–434.
[10] K.C. Cheng, D.S. Cahill, H. Kasai, S. Nishimura, L.A. Loeb, 8-Hydroxyguanine, an abundant form of oxidative DNA damage, causes G → T and A → C substitutions, J. Biol. Chem. 267 (1992) 166–172.
[11] S. Asami, T. Hirano, R. Yamaguchi, Y. Tomioka, H. Itoh, H. Kasai, Increase of a type of oxidative DNA damage, 8-hydroxyguanine, and its repair activity in human leukocytes by cigarette smoking, Cancer Res. 56 (1996) 2546–2549.
[12] R. Yamaguchi, T. Hirano, S. Asami, A. Sugita, H. Kasai, Increase in the 8-hydroxyguanine repair activity in the rat kidney after the administration of a renal carcinogen, ferric nitrilotriacetate, Environ. Health Perspect. 104 (1996) 651–653.
[13] R. Yamaguchi, T. Hirano, S. Asami, K.M. Chung, A. Sugita, H. Kasai, Increased 8-hydroxyguanine levels in DNA and its repair activity in rat kidney after administration of a renal carcinogen, ferric nitrilotriacetate, Carcinogenesis 17 (1996) 2419–2422.
[14] T. Hirano, Y. Yamaguchi, H. Kasai, Inhibition of 8-hydroxyguanine repair in testes after administration of cadmium chloride to GSH-depleted rats, Toxicol. Appl. Pharmacol. 147 (1997) 9–14.
[15] R. Yamaguchi, T. Hirano, Y. Ootsuyama, S. Asami, Y. Tsurudome, S. Fukada, H. Yamato, T. Tsuda, I. Tanaka, H. Kasai, Increased 8-hydroxyguanine in DNA and its repair activity in hamster and rat lung after intratracheal instillation of crocidolite asbestos, Jpn. J. Cancer Res. 90 (1999) 505–509.
[16] Y. Tsurudome, T. Hirano, H. Yamato, I. Tanaka, M. Sagai, H. Hirano, N. Nagata, H. Itoh, H. Kasai, Changes in levels of 8-hydroxyguanine in DNA, its repair and

OGG1 mRNA in rat lungs after intratracheal administration of diesel exhaust particles, Carcinogenesis 20 (1999) 1573–1576.
[17] T. Hirano, K. Higashi, A. Sakai, Y. Tsurudome, Y. Ootsuyama, R. Kido, H. Kasai, Analyses of oxidative DNA damage and its repair activity in the livers of 3′-methyl-4-dimethylaminoazobenzene-treated rodents, Jpn. J. Cancer Res. 91 (2000) 681–685.
[18] N. Mei, N. Kunugita, T. Hirano, H. Kasai, Acute arsenite-induced 8-hydroxyguanine is associated with inhibition of repair activity in cultured human cells, Biochem. Biophys. Res. Commun. 297 (2002) 924–930.
[19] N. Mei, K. Tamae, N. Kunugita, T. Hirano, H. Kasai, Analysis of 8-hydroxydeoxyguanosine 5′-monophosphate (8-OH-dGMP) as a reliable marker of cellular oxidative DNA damage after gamma-irradiation, Environ. Mol. Mutagen. 41 (2003) 332–338.
[20] T. Hirano, Y. Yamaguchi, H. Hirano, H. Kasai, Age-associated change of 8-hydroxyguanine repair activity in cultured human fibroblasts, Biochem. Biophys. Res. Commun. 214 (1995) 1157–1162.
[21] T. Hirano, R. Yamaguchi, S. Asami, N. Iwamoto, H. Kasai, 8-Hydroxyguanine levels in nuclear DNA and its repair activity in rat organs associated with age, J. Gerontol. A51 (1996) B303–B307.
[22] Y. Tsurudome, T. Hirano, K. Hirata, A. Higure, N. Nagata, K. Takahashi, H. Itoh, H. Kasai, Age associated increase of 8-hydroxydeoxyguanosine in human colorectal tissue DNA, J. Gerontol. 56A (2001) B483–485.
[23] S. Asami, T. Hirano, R. Yamaguchi, Y. Tsurudome, H. Itoh, H. Kasai, Effects of forced and spontaneous exercise on 8-hydroxydeoxyguanosine levels in rat organs, Biochem. Biophys. Res. Commun. 243 (1998) 678–682.
[24] T. Hirano, K. Kawai, Y. Ootsuyama, H. Kasai, Fragmentation of the DNA repair enzyme, OGG1, in mouse nonparenchymal liver cells by arsenic compounds, Genes Environ. 28 (2006) 62–67.
[25] R.J. Potts, R.D. Watkin, B.A. Hart, Cadmium exposure down-regulates 8-oxoguanine DNA glycosylase expression in rat lung and alveolar epithelial cells, Toxicology 184 (2003) 189–202.
[26] C.K. Youn, S.H. Kim, D.Y. Lee, S.H. Song, I.Y. Chang, J.W. Hyun, M.H. Chung, H.J. You, Cadmium down-regulates human OGG1 through suppression of Sp1 activity, J. Biol. Chem. 280 (2005) 25185–25195.
[27] N.J. Hodges, J.K. Chipman, Down-regulation of the DNA-repair endonuclease 8-oxo-guanine DNA glycosylase 1 (hOGG1) by sodium dichromate in cultured human A549 lung carcinoma cells, Carcinogenesis 23 (2002) 55–60.
[28] A.J. Lee, N.J. Hodges, J.K. Chipman, Interindividual variability in response to sodium dichromate-induced oxidative DNA damage: role of the $Ser^{326}Cys$ polymorphism in the DNA-repair protein of 8-oxo-7, 8-dihydro-2′-deoxyguanosine DNA glycosylase 1, Cancer Epidemiol. Biomarkers Prev. 14 (2005) 497–505.
[29] V. Sava, D. Mosqouera, S. Song, F. Cardozo-Pelaez, J.R. Sánchez-Ramos, Effects of melanin and manganese on DNA damage and repair in PC12-derived neurons, Free Rad. Biol. Med. 36 (2004) 1144–1154.
[30] J. Sanchez-Ramos, E. Overvik, B.N. Ames, A marker of oxyradical-mediated DNA damage (oxo8dG) is increased in nigrostriatum of Parkinson's disease brain, Neurodegeneration (Exp. Neurol.) 3 (1994) 197–204.
[31] K. Bialkowski, A. Bialkowska, K.S. Kasprzak, Cadmium(II), unlike nickel(II), inhibits 8-OH-dGTPase activity and increases 8-OH-dG level in DNA of the rat testis, a target organ for cadmium(II) carcinogenesis, Carcinogenesis 20 (1999) 1621–1624.
[32] IARC, Chromium, Nickel, Welding. IARC Monographs, vol. 49, IARC, Lyon, 1990.
[33] IARC, Beryllium, Cadmium, Mercury and Exposures in the Glass Manufacturing Industry. IARC Monographs, vol. 58, IARC, Lyon, 1993.
[34] H. Dalley, A. Hartwig, Induction and repair inhibition of oxidative DNA damage by nickel(II) and cadmium(II) in mammalian cells, Carcinogenesis 18 (1997) 1021–1026.
[35] H. Merzenich, A. Hartwig, W. Ahrens, D. Beyersmann, R. Schlepegrell, M. Scholze, J. Timm, K.H. Jöckel, Biomonitoring on carcinogenic metals and oxidative DNA damage in a cross-sectional study, Cancer Epidemiol. Biomark. Prev. 10 (2001) 515–522.
[36] J.G. Hengstler, U. Bolm-Audorff, A. Faldum, K. Janssen, M. Reifenrath, W. Götte, D. Jung, O. Mayer-Popken, J. Fuchs, S. Gebhard, H.G. Bienfait, K. Schlink, C. Dietrich, D. Faust, B. Epe, F. Oesch, Occupational exposure to heavy metals: DNA damage induction and DNA repair inhibition prove co-exposures to cadmium, cobalt and lead as more dangerous than hitherto expected, Carcinogenesis 24 (2003) 63–73.
[37] T. Suzuki, M. Honda, S. Matsumoto, S.R. Stüzenbaum, S. Gamou, Valosine-containing proteins (VCP) in an annelid: identification of a novel spermatogenesis related factor, GENE 362 (2005) 11–18.
[38] S.M. Hsu, L. Raine, H. Fanger, A comparative study of the peroxidase–anti-peroxidase method and an avidin–biotin complex method for studying the polypeptide hormones with radioimmunoassay antibodies, Am. J. Clin. Pathol. 75 (1981) 734–738.
[39] Y. Hattori, C. Nishigori, T. Tanaka, K. uchida, O. Nikaido, T. Osawa, H. Hiai, S. Imamura, S. Toyokuni, 8-Hydroxy-2′-deoxyguanosine is increased in epidermal cells of hairless mice after chronic ultraviolet B exposure, J. Invest. Dermatol. 107 (1997) 733–737.
[40] K. Kawai, Y.S. Li, H. Kasai, Accurate measurement of 8-OH-dG and 8-OH-Gua in mouse DNA, urine and serum: effects of X-ray irradiation, Genes Environ. 29 (2007) 107–114.
[41] J.E. Morgan, A.J. Morgan, Earthworms as biological monitors of cadmium, copper, lead and zinc in metalliferous soils, Environ. Pollut. 54 (1988) 123–138.
[42] M.G. Burgos, C. Winters, S.R. Stürzenbaum, P.F. Randerson, P. Kille, A.J. Morgan, Cu and Cd effects on the earthworm *Lumbricus rubellus* in the laboratory: multivariate statistical analysis of relationships between exposure, biomarkers, and ecologically relevant parameters, Environ. Sci. Technol. 39 (2005) 1757–1763.
[43] J.K. Saxe, C.A. Impellitteri, W.J. Peijnenburg, H.E. Allen, Novel model describing trace metal concentrations in the earthworm, *Eisenia andrei*, Environ. Sci. Technol. 35 (2001) 4522–4529.
[44] M.G. Vijver, H.T. Wolterbeek, J.P. Vink, C.A. van Gestel, Surface adsorption of metals onto the earthworm *Lumbricus rubellus* and the isopod *Porcellio scaber* is negligible compared to absorption in the body, Sci. Total Environ. 340 (2005) 271–280.
[45] T.P. Coogan, N. Shiraishi, M.P. Waalkes, Minimal basal activity and lack of metal-induced activation of the metallothionein gene correlates with lobe-specific sensitivity to the carcinogenic effects of cadmium in the rat prostate, Toxicol. Appl. Pharmacol. 132 (1995) 164–173.
[46] G. Xu, G. Zhou, T. Jin, T. Zhou, S. Hammarstrom, A. Bergh, G. Nordberg, Apoptosis and p53 gene expression in male reproductive tissues of cadmium exposed rats, Biometals 12 (1999) 131–139.
[47] S.R. Stürzenbaum, P. Kille, A.J. Morgan, The identification, cloning and characterization of earthworm metallothionein, FEBS Lett. 431 (1998) 437–442.
[48] C.J. Langdon, C. Winters, S.R. Stürzenbaum, A.J. Morgan, J.M. Charnock, A.A. Meharg, T.G. Pearce, P.H. Lee, K.T. Semple, Ligand arsenic complexation and immunoperoxidase detection of metallothionein in the earthworm *Lumbricus rubellus* inhabiting arsenic-rich soil, Environ. Sci. Technol. 39 (2005) 2042–2048.

See related commentary on pg 2138

ORIGINAL ARTICLE

UVA1 Genotoxicity Is Mediated Not by Oxidative Damage but by Cyclobutane Pyrimidine Dimers in Normal Mouse Skin

Hironobu Ikehata[1], Kazuaki Kawai[2], Jun-ichiro Komura[1], Ko Sakatsume[1], Liangcheng Wang[1], Masaru Imai[3], Shoichi Higashi[4], Osamu Nikaido[5], Kazuo Yamamoto[3], Kotaro Hieda[6], Masakatsu Watanabe[4], Hiroshi Kasai[2] and Tetsuya Ono[1]

UVA1 induces the formation of 8-hydroxy-2′-deoxyguanosines (8-OH-dGs) and cyclobutane pyrimidine dimers (CPDs) in the cellular genome. However, the relative contribution of each type of damage to the *in vivo* genotoxicity of UVA1 has not been clarified. We irradiated living mouse skin with 364-nm UVA1 laser light and analyzed the DNA damage formation and mutation induction in the epidermis and dermis. Although dose-dependent increases were observed for both 8-OH-dG and CPD, the mutation induction in the skin was found to result specifically from the CPD formation, based on the induced mutation spectra in the skin genome: the dominance of C→T transition at a dipyrimidine site. Moreover, these UV-specific mutations occurred preferentially at the 5′-TCG-3′ sequence, suggesting that CpG methylation and photosensitization-mediated triplet energy transfer to thymine contribute to the CPD-mediated UVA1 genotoxicity. Thus, it is the CPD formation, not the oxidative stress, that effectively brings about the genotoxicity in normal skin after UVA1 exposure. We also found differences in the responses to the UVA1 genotoxicity between the epidermis and the dermis: the mutation induction after UVA1 irradiation was suppressed in the dermis at all levels of irradiance examined, whereas it leveled off from a certain high irradiance in the epidermis.

Journal of Investigative Dermatology (2008) **128**, 2289–2296; doi:10.1038/jid.2008.61; published online 20 March 2008

INTRODUCTION

Sunlight reaching the earth's surface contains UV radiation consisting of UVB (290–320 nm) and UVA (320–400 nm). Although the UVB component is known to include the most carcinogenic wavelengths for mammalian skin (De Gruijl and Van der Leun, 1994), the UVA component is also suggested to play an important role in the skin genotoxicity of solar UV (Setlow *et al.*, 1993). The genotoxicity of UVB derives from its potent mutagenicity through the photochemical formation of specific types of DNA base damage such as cyclobutane pyrimidine dimers (CPDs) and pyrimidine(6-4)pyrimidone photoproducts (64PPs) after direct absorption of the photon energy to DNA molecules (Friedberg *et al.*, 2005). UVA genotoxicity for mammalian cells depends on the wavelength: at a shorter wavelength range (320–340 nm), the UVA2 region, the effect is exerted mainly through the same direct photochemical reaction with DNA as that by UVB, although its efficiency is very low (Kielbassa and Epe, 2000; Ikehata and Ono, 2007), whereas indirect genotoxic effects also occur through the production of reactive oxygen species (ROS) by photosensitization of biological molecules other than DNA, especially in the longer wavelength range of UVA1 (340–400 nm) (Kvam and Tyrrell, 1997; Kielbassa and Epe, 2000; Tyrrell, 2000).

The significance of the indirect oxidative damage-mediated genotoxicity of UVA for the mammalian genome, however, has been controversial. Although several studies supported the ROS-mediated genotoxicity of UVA (Besaratinia *et al.*, 2004, 2007; Wood *et al.*, 2006), studies showing a major contribution of CPD, which can be induced in cellular DNA directly or indirectly by UVA (Courdavault *et al.*, 2004), have also been reported (Ikehata *et al.*, 2003a), even within the UVA1 range (Van Kranen *et al.*, 1997; Kappes *et al.*, 2006). In addition, another DNA modification by UVA was also suggested in previous studies (Drobetsky *et al.*, 1995;

[1]*Department of Cell Biology, Graduate School of Medicine, Tohoku University, Sendai, Japan;* [2]*Department of Occupational Oncology, Institute of Industrial Ecological Sciences, University of Occupational and Environmental Health, Kitakyushu, Japan;* [3]*Department of Biomolecular Sciences, Graduate School of Life Sciences, Tohoku University, Sendai, Japan;* [4]*National Institutes of Natural Sciences, National Institute for Basic Biology, Okazaki, Japan;* [5]*Department of Food and Nutrition, Kanazawa Gakuin College, Kanazawa, Japan and* [6]*Department of Life Science, Rikkyo University, Tokyo, Japan*

Correspondence: Dr Hironobu Ikehata, Division of Genome and Radiation Biology, Department of Cell Biology, Graduate School of Medicine, Tohoku University, Seiryo-machi 2-1, Aoba-ku, Sendai 980-8575, Japan.
E-mail: ikehata@mail.tains.tohoku.ac.jp

Abbreviations: CPD, cyclobutane pyrimidine dimer; 8-OH-dG, 8-hydroxy-2′-deoxyguanosine; MF, mutant frequency; 64PP, pyrimidine(6-4)pyrimidone photoproduct; ROS, reactive oxygen species

Received 9 November 2007; revised 22 January 2008; accepted 9 February 2008; published online 20 March 2008

Agar *et al.*, 2004), and this modification specifically induced a rare type of transversion mutation, T→G, which was referred to as the UVA fingerprint in those studies, although the DNA lesions or mechanisms causing the mutation have not been established. Discrepancies in the types of UVA genotoxicity among those studies may have resulted in part from differences in the UVA source used in each study: the inclusion of a shorter wavelength component in the emitted UVA could, even if it is very small, modify or overwhelm the resultant mutation spectrum with a UVB-like profile. However, attention should be given to the experimental conditions during the cellular exposure to UVA, because ROS production by irradiation can be influenced profoundly by the cellular environment such as the ingredients in the cultured media and oxygen concentration, which could mediate the indirect genotoxicity of UVA as photosensitizers or effectors (Besaratinia *et al.*, 2007). As long as cells are cultured in artificial conditions, such ambiguities concerning the causes of the UVA genotoxicity cannot be resolved.

To exclude such problems that are intrinsic to cultured cell systems, we employed *in vivo* analysis of UVA genotoxicity, in which transgenic mice developed for mutation research were irradiated and the induced mutations were evaluated directly in the exposed skin (Ikehata *et al.*, 2003a). The induced mutation spectrum observed in the epidermis was rather similar to that induced by UVB, which we determined previously (Ikehata *et al.*, 2003b), although much more remarkable hot spots for UV-specific C→T transitions appeared at methylated CpG-associated dipyrimidine sites after UVA irradiation (Ikehata *et al.*, 2003a). However, the UVA source used in that study emitted not only UVA1 but also UVA2 and even a small amount of the boundary wavelengths of UVB, which might have affected the results. In this study, we used a laser emitting a purely monochromatic 364-nm UV light to avoid the problem of contamination by shorter wavelengths, and analyzed the mutation spectrum as well as the DNA lesions induced in the exposed mouse skin.

RESULTS

Induction of DNA damage in skin

A significant dose-dependent increase in the amount of 8-hydroxy-2′-deoxyguanosine (8-OH-dG) in genomic DNA was observed in both the epidermis and dermis of mouse skin ($P<0.0001$, two-way analysis of variance) after exposure to 0.85–3 MJ m^{-2} of the 364-nm UVA1 light (Figure 1a), confirming a genotoxic effect on the skin through the UVA1-mediated production of ROS, which should then oxidize the cellular DNA to produce oxidative damage represented by 8-OH-dG (Kvam and Tyrrell, 1997; Kielbassa and Epe, 2000; Tyrrell, 2000). Simultaneously, a significant linear increase in the amount of CPD along with the increase in UVA1 irradiance was also observed in both the tissues ($P<0.0001$, two-way analysis of variance), whereas no significant induction of 64PP was detected in either tissue at any level of irradiance examined (Figure 1b). These amounts of CPD produced after the UVA1 irradiation were quite comparable to those of the photolesions induced with 0.5 kJ m^{-2} of UVB (Figure 1b), a dose sufficient to induce mutations at more than 10-fold the background level and the minimal dose provoking inflammation in mouse skin (Ikehata and Ono, 2002), indicating that the amounts of CPD

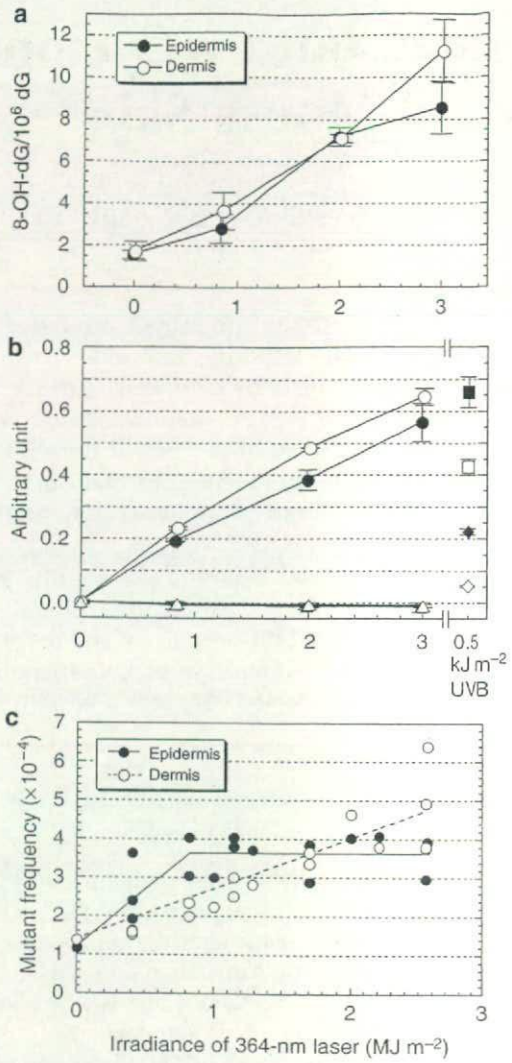

Figure 1. Genotoxic effects of 364-nm UVA1 on mouse epidermis and dermis. (**a**) Dose-dependent production kinetics of 8-OH-dG in the epidermis (closed circles) and dermis (open circles) after UVA1 irradiation. The amounts of 8-OH-dG in the genomic DNA from each tissue were quantified with an HPLC/electrochemical detector system. Data points were obtained from two to three mice for each dose. (**b**) Dose-dependent induction kinetics of CPD (circles) and 64PP (triangles) in the epidermis (closed symbols) and dermis (open symbols) after UVA1 irradiation. For comparison, the amounts of CPD (squares) and 64PP (diamonds) induced after 0.5 kJ m^{-2} UVB are given on the right side. The amounts of the photolesions were evaluated with an ELISA using specific mAbs. Each set of data points was obtained from two mice. (**c**) Dose-dependent induction kinetics of MF of the *lacZ* transgene in the epidermis (closed circles) and dermis (open circles) after UVA1 irradiation. Each data point was from a single animal. Regression lines are given for the epidermal data points less than 1 MJ m^{-2} (solid line, $R^2=0.934$, $P<0.001$) and for all the dermal points (dotted line, $R^2=0.932$, $P<0.0001$) under the presumption that the *y*-intercept equals the background MF. For the data points of epidermis over 0.8 MJ m^{-2}, a horizontal solid line is drawn at the mean of those data ($3.64\pm0.47\times10^{-4}$), which is significantly different from the background MF ($P<0.0001$), to show the suppression of MF induction.

produced at these levels of UVA1 irradiance would be enough to exert genotoxicity in the skin. In contrast to UVB, UVA1 induced similar amounts of CPDs in the epidermis and dermis (Figure 1b), and a similar situation was also observed for the amounts of 8-OH-dG (Figure 1a), probably reflecting the high penetration of the epidermis by wavelengths >300-nm UV (Bruls *et al.*, 1984) and the thinness of the mouse epidermis.

Mutation induction in skin

Sixteen mice were exposed to the 364-nm UVA1 light at irradiances of 0.41–2.56 MJ m^{-2}, and the frequencies of the mutations induced in the epidermis and dermis were evaluated 4 weeks later using the *lacZ* transgene as a mutational reporter. The observed mutant frequencies (MFs) are plotted in Figure 1c along with the background MFs (1.18×10^{-4} for the epidermis and 1.38×10^{-4} for the dermis; Ikehata and Ono, 2002). A significant dose-dependent linear increase in MF was observed in the dermis at the entire dose range examined (regression analysis: slope $= 1.32 \times 10^{-10}$ per Jm^{-2}, $R^2 = 0.932$, $P < 0.0001$), and in the epidermis at doses up to 0.82 MJ m^{-2} (slope $= 2.97 \times 10^{-10}$ per Jm^{-2}, $R^2 = 0.934$, $P < 0.001$). The slopes were significantly different between the two tissues ($P < 0.001$): 2.3-fold steeper in the epidermis. However, at doses more than 0.82 MJ m^{-2}, the MF increase in the epidermis was suppressed almost completely to a constant level of MF: mean $= 3.64(\pm 0.47) \times 10^{-4}$ ($n = 13$), which was still significantly higher than the background MF (3.1-fold, $P < 0.0001$). During the experiments, we noticed inflammation in the exposed skin area in all the mice 2 days after the irradiation, even at the smallest irradiance examined (0.41 MJ m^{-2}).

UVA1-induced mutation spectrum in the epidermis

In total, 147 *lacZ* mutants were isolated from the epidermis of six mice exposed to 1.00–2.56 MJ m^{-2} of 364-nm UVA1. The entire coding region of the *lacZ* gene of these mutants was sequenced, and mutations were detected for all the mutants (Table S1). We found that 92% ($n = 134$) of these mutants had a single-base substitution. The others were five mutants with a frameshift, two with a complex mutation, which is a frameshift associated with base changes, four with a deletion, and two with an identical 1.3-kb insertion. The last two mutants were excluded from further analysis because their insertion included a bacterial transposable element and most likely resulted from an *ex vivo* mutation that occurred during recovery of the transgene. The same insertion mutation was recovered and characterized in our previous study (Ikehata *et al.*, 2007b). The obtained mutation spectrum for the UVA1-exposed epidermis is summarized in Table 1, and compared with the UVB-induced and background spectra, which we reported before (Ikehata *et al.*, 2003b).

Among the 134 mutants with a single-base substitution recovered in the irradiated epidermis, 94 (65% of total mutants) were C→T transition, 90% of which ($n = 85$) occurred at dipyrimidine sites, where UV photolesions are preferentially produced. In contrast to the high recovery of these UV-specific mutations of C→T at dipyrimidine sites, G→T transversion, which is known to be one of the most representative ROS-induced mutations and to result from 8-OH-dG (Grollman and Moriya, 1993), was recovered as a minor fraction ($n = 11$, 8%), and no T→G base substitution, the UVA fingerprint mutation (Drobetsky *et al.*, 1995), was detected (Table 1). We also analyzed the DNA sequence changes in the *lacZ* mutants recovered from the dermis of the UVA1-exposed skin, and found a mutation spectrum similar to that in the epidermis: a dominance of the UV-specific mutation and small numbers of the ROS-specific and UVA fingerprint mutations (data not shown).

The mutation spectrum observed in the UVA1-exposed epidermis was significantly different from that in the UVB-exposed epidermis (Table 1; $P < 0.001$, Adams–Skopek test). The difference seems to result mainly from the larger ratio of C→T transitions in the UVB spectrum than in the UVA1 spectrum (85 vs 65%) and especially from the more frequent occurrences of those C→T mutations at non-CpG sites in the UVB spectrum (39 at non-CpG/65 total for UVB vs 14/94 for

Table 1. Summary of mutation spectra in mouse skin epidermis

	364-nm UVA1		UVB[1]		Background[1]	
	Number (%)	% (Py-Py)[2]	Number (%)	% (Py-Py)[2]	Number (%)	% (Py-Py)[2]
Base substitution	134 (92)		75 (97)		42 (95)	
Transition						
C→T (CpG)	80 (55)	93	26 (34)	96	24 (55)	63
C→T (non-CpG)	14 (10)	79	39 (51)	100	2 (5)	50
T→C	25 (17)	0	1 (1)	100	6 (14)	0
Transversion						
G→C	1 (1)	100	2 (3)	100	1 (2)	0
G→T	11 (8)	55	1 (1)	100	5 (11)	80
T→G					1 (2)	0
T→A	3 (2)	100	4 (5)	100	2 (5)	100
Tandem			2 (3)	100	1 (2)	100
Frameshift	5 (3)	60	2 (3)	50	1 (2)	0
Complex[3]	2 (1)	75*				
Duplication					1 (2)	
Deletion	4 (3)					
Total	145		77		44	

Py, Pyrimidine.
[1]Ikehata *et al.* (2003b).
[2]Percentage of the fraction of the mutations that occurred at dipyrimidine sites.
[3]Frameshift mutations associated with base changes.
*For one of the two mutations, only one nucleotide of the affected dinucleotide resided in a dipyrimidine site.

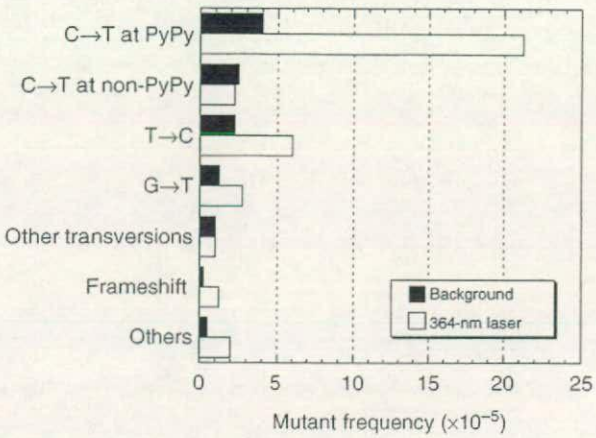

Figure 2. Comparison of the frequencies of mutants with each class of mutations in the epidermis between unirradiated (background) and UVA1-irradiated (364-nm laser) mice. The MF of each class was calculated by multiplying the observed overall MF (1.18×10^{-4} for the background and 3.64×10^{-4} for the irradiated) with the fraction of the class in overall mutations. PyPy, a dipyrimidine site.

UVA1; Table 1). On the contrary, the UVA1 spectrum was not significantly different from that in the unirradiated epidermis (the background shown in Table 1) for both overall and base substitution mutations (Adams–Skopek test), probably reflecting in part the low level of MF induction by UVA1. However, a significant difference was detected when the numbers of UV-specific and non-UV-specific C→T transitions, which differ in association with dipyrimidine sites, were compared between the unirradiated (16 and 10) and the irradiated (85 and 9) epidermis ($P<0.005$, Fisher's exact probability test), reflecting the more frequent occurrence of C→T mutations at dipyrimidine sites in the exposed epidermis (90%) than in the unirradiated epidermis (62%) (see also Table 1). Furthermore, the frequency of mutants with each class of mutations was calculated from the overall MFs and its proportion in the mutation spectra, and was compared between the background and the induced mutations, as shown in Figure 2, which clearly demonstrated that the observed MF increase in the epidermis after 364-nm UVA1 irradiation mainly resulted from the induction of UV-specific C→T transitions but not 8-OH-dG-mediated G→T or other transversion mutations. Although we detected both CPD and 8-OH-dG induction in mouse skin by UVA1, these results indicate that only CPD, which is known to induce UV-specific mutations (Tessman *et al.*, 1992), can effectively bring about genotoxicity in the skin after UVA1 irradiation and that the amount of 8-OH-dG produced simultaneously would not appear to be enough to harm the skin genome, at least in normal mice whose response to ROS-induced DNA lesions should not be compromised.

Characterization of UVA1-induced mutations

To investigate the preferred DNA sequence contexts for the UV-specific C→T transitions induced in UVA1-exposed mouse epidermis, all the cytosine residues in dipyrimidine sites on both strands of the *lacZ*-coding region were categorized into 12 groups based on their surrounding sequence context as shown in Table 2, in which the cytosine subjected to the mutation was located at the middle position of triplet sequences that include dipyrimidines. Sites for the UVA1-induced UV-specific mutation were found most frequently in the 5′-TCG-3′ context (see the mutabilities in context in Table 2), and an outstanding number of mutants with the mutation were also recovered in the same sequence context ($n=70$; see the number of mutants in Table 2). Moreover, the mutation-detected sites with the 5′-TCG-3′ context seemed to produce the UV-specific mutations much more frequently than those with other contexts, as evidenced by the average recurrences in Table 2 (7.78 vs 1.00–2.00). These estimations indicate that the UV-specific C→T transition induced by UVA1 occurs most preferably in the 5′-TCG-3′ sequences.

This association of UVA1-induced mutations with the 5′-TCG-3′ sequence context suggests the importance of cytosine methylation at CpG sites (Grünwald and Pfeifer, 1989) for UVA1 mutagenesis in the mammalian genome, as it has been shown that transgenes of the mice used here are fully methylated in the skin (Ikehata *et al.*, 2003b). When examining the distribution in the *lacZ* coding sequence of mutations recovered from the UVA1-exposed epidermis (Figure 3), almost all of the C→T mutations at 5′-TCG-3′ sites (69/70) were found to occur repeatedly at several certain positions in the gene, some of which showed hot spots for this mutation type (positions 928, 1,187, 1,627, and 2,392). This observation suggests that UVA1-mediated genotoxicity in mammalian skin depends on CpG methylation. In the distribution, another hot spot, where T→C transitions occurred exclusively, was noticed at position 625 (Figure 3). The same outstanding hot spot was also observed in the distribution of the background mutations, as shown before (Ikehata *et al.*, 2003b), indicating that these hot spot mutations would occur spontaneously, not by UVA exposure.

DISCUSSION

After 364-nm UVA1 irradiation, we observed the induction of 8-OH-dG and CPD but not of 64PP in both the epidermis and dermis of living mice. The simultaneous formation of 8-OH-dG and CPD without 64PP induction by UVA1 was also reported in cultured cells (Kielbassa and Epe, 2000; Courdavault *et al.*, 2004; Besaratinia *et al.*, 2005) and skin specimens (Mouret *et al.*, 2006). The 8-OH-dG formation would result from DNA oxidation by ROS produced through UVA-mediated photosensitization of intrinsic biomolecules such as riboflavin and porphyrin (Tyrrell, 2000; Besaratinia *et al.*, 2007). For the CPD production, there are two possible pathways: one is a photochemical reaction through the direct absorption of UVA1 energy to DNA, and the other is an indirect triplet energy transfer mediated by some photosensitized molecules (Lamola, 1970), although the identity of those mediators is currently not known. The absence of 64PP induction favors the latter possibility because direct energy transfer by the former mechanism should have produced 64PPs equally, although the photochemical conversion to Dewar valence isomers

Table 2. Influence of adjacent bases on UV-specific C→T mutations induced by 364-nm UVA1

	Number of sites in the *lacZ* coding					
Sequence context[1]	All	Mutable[2]	Detected[3]	Number of mutants	Mutability in context[4]	Average recurrence[5]
5′-TCA-3′	112	71	1	1	0.01	1.00
5′-CCA-3′	139	100	2	2	0.02	1.00
5′-TCG-3′	113	74	9	70	0.12	7.78
5′-CCG-3′	152	99	3	4	0.03	1.33
5′-ACT-3′	64	24	0	0	<0.04	—
5′-ACC-3′	112	88	1	2	0.01	2.00
5′-GCT-3′	121	53	0	0	<0.02	—
5′-GCC-3′	148	119	0	0	<0.01	—
5′-TCT-3′	52	20	1	2	0.05	2.00
5′-TCC-3′	91	62	2	3	0.03	1.50
5′-CCT-3′	60	24	1	1	0.04	1.00
5′-CCC-3′	71	57	0	0	<0.02	—

[1]Either base adjacent to the 5′ or 3′ side of the cytosine that should be subject to mutation to thymine is shown. Tandem pyrimidines are underlined.
[2]Sites where an amino-acid change or termination is expected if a C→T transition occurs.
[3]Sites where C→T transitions were detected for 364-nm UVA1-irradiated skin epidermis.
[4]Numbers of detected sites were divided by numbers of the mutable sites of the same sequence context.
[5]Numbers of mutants were divided by numbers of the detected sites of the same sequence context.

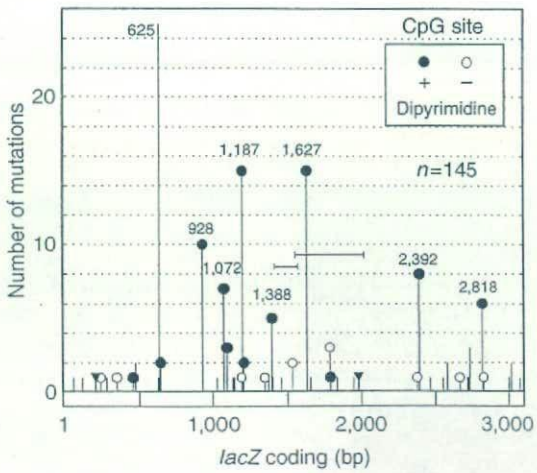

Figure 3. Distribution in the *lacZ* transgene of mutations detected in 364-nm UVA1-exposed mouse skin epidermis. The horizontal open bar indicates positions in the *lacZ* coding sequence. The number of mutations at each position is shown by vertical lines above the horizontal bar. The positions at which cytosine mutations were detected within Py-CpG and Pu-CpG sequences are shown by closed and open lollipops, respectively (Py, pyrimidine; Pu, purine). The sites for small (<20 bp) and large (>100 bp) deletions are indicated by reverse triangles and horizontal lines with short vertical lines on their ends, respectively. Position numbers are given for recurrent sites at which more than four identical mutations were detected.

might have precluded the detection of such 64PPs. A study with HPLC coupled with tandem mass spectrometry, however, showed no formation of 64PPs and Dewar isomers in cellular DNA after UVA1 irradiation (Courdavault *et al.*, 2004), and reported a preferential CPD formation at TT dipyrimidines (Courdavault *et al.*, 2004; Mouret *et al.*, 2006), which also supports the indirect triplet energy transfer mechanism because the energy level of the excited triplet state of thymine is the lowest among DNA bases. In addition, we observed the induction of similar but significantly larger amounts of CPD in the dermis compared to the epidermis after UVA1 irradiation ($P<0.05$, two-way analysis of variance; Figure 1b), which might suggest a biased distribution of some unidentified photosensitizers toward the dermis because, if the direct energy absorption reaction were relevant, the amounts of CPD should be larger in the epidermis, even if the difference is very small due to the high penetration of UVA1 into the skin. Moreover, an action spectrum of CPD formation in naked and cellular DNA previously reported showed a shoulder at the UVA1 wavelength range (Matsunaga *et al.*, 1991; Kielbassa and Epe, 2000), suggesting some photochemical reaction producing CPDs that was different from the direct energy transfer mechanism that peaks at 260 nm. These observations favor the photosensitized triplet energy transfer pathway for the CPD formation mechanism by UVA1.

Although we observed 8-OH-dG formation in the skin genome with UVA1 irradiation, there was no evidence that it significantly contributed to the genotoxicity in the skin in the following mutation studies (Table 1 and Figure 2). This result may suggest that the ability of normal mouse skin to repair ROS-mediated DNA damage is high enough to suppress the mutagenicity of such DNA lesions, which is consistent with previous studies reporting fast and efficient repair of 8-OH-dG in cultured normal keratinocytes and fibroblasts (Klungland *et al.*, 1999; Orimo *et al.*, 2006). In those studies, 50% of 8-OH-dGs were removed from the cellular genome

within 6 hours, a time length in which no significant repair of CPD was observed in cells and skin tissues of mice (Mizuno *et al.*, 1991; Ikehata *et al.*, 2007a). Apoptotic responses to ROS-induced DNA damage or to ROS itself might also be related to the suppression of genotoxicity. Nevertheless, because we used only a single wavelength within the UVA1 range in this study, it could be suggested that the amount of 8-OH-dG, in other words the abundance of ROS, induced here was not large enough to reflect the real situation under actual solar UVA. This would not be the case, however, as the observed amounts of 8-OH-dG induced after the 364-nm UVA1 (4–10 molecules per 10^6 deoxyguanosines; Figure 1a) were nearly equal to those observed in studies with broadband UVA1 sources (Besaratinia *et al.*, 2005; Mouret *et al.*, 2006). Thus, the ROS induced after UVA1 irradiation would not seem to be potent enough to cause genotoxicity in normal cells or skin, even if the irradiance is above the maximal physiological level of daily UVA from natural sunlight ($\leqslant 1.5\,MJ\,m^{-2}$).

The sequence analysis of mutants in this study clearly showed that the mutation induction by UVA1 exposure was mediated mainly by CPD formation in both the epidermis and dermis. However, the initial increments in MF were 2.3-fold larger in the epidermis than in the dermis, although similar amounts of CPD were produced in both tissues at each level of irradiance examined (Figure 1b and c). This apparent inconsistency may suggest some differences in the response to UVA1 between the epidermis and the dermis. One possibility is that DNA repair for CPDs is more active or efficient in the dermis than in the epidermis. Although it has been reported that keratinocytes *in vitro* show a higher level of CPD removal than skin fibroblasts after UVB irradiation (D'Errico *et al.*, 2003), the difference in cell proliferation rates *in vivo* between the two tissues could contribute to the situation: if fibroblasts proliferate in skin tissue after irradiation much more slowly than keratinocytes, more repair time would be available to the fibroblasts, resulting in more efficient DNA repair in the dermis. Another possibility is that the fibroblasts in the dermis are more sensitive to UVA1 genotoxicity than the keratinocytes in the epidermis because of some cell-exclusion responses such as apoptosis, which could lead to more efficient exclusion of damaged cells from the dermis than from the epidermis, with the result that the remaining cells in the dermis show fewer mutations. Consistent with this idea, higher sensitivities to UVA1-mediated cell killing have been demonstrated for dermal fibroblasts than for keratinocytes (Leccia *et al.*, 1998; Courdavault *et al.*, 2004).

Furthermore, at a higher dose range than $0.8\,MJ\,m^{-2}$, the mutation induction in the epidermis seemed to be repressed completely, although the amount of CPD in the tissue continued to increase lineally with the increase in UVA1 irradiance (Figure 1b and c). This observation might suggest some antigenotoxic response specific to the epidermis, which should be different from the mutation-suppressing response observed in the dermis mentioned above, because the mutation suppression kinetics were quite different between the two tissues: the slope was suppressed at all irradiances for the dermis, whereas it leveled off from a certain high-dose point in the epidermis (Figure 1c). A level-off kinetics of mutation induction was also reported previously for the epidermis of UVB-exposed mice (Ikehata and Ono, 2002), which may indicate that this level-off response to mutation induction is epidermis specific and acts in response to multiple environmental genotoxic agents, including UVB and UVA1, although the mechanism of this response remains unknown. Interestingly, the level-off response appears at a lower MF for UVA1 (3.64×10^{-4}) than for UVB (18.10×10^{-4}) (Ikehata and Ono, 2002). This difference might explain the observation in a skin carcinogenesis study with hairless mice that UVA1 carcinogenesis was less dose dependent than UVB carcinogenesis (De Laat *et al.*, 1997), because, irrespective of the given doses, the genotoxic effect at a single exposure would be smaller with UVA1 than with UVB.

We found that UVA1 caused UV-specific C→T transitions most frequently and that these mutations occurred preferentially at 5′-TCG-3′ sequences (Tables 1 and 2) forming hot spots at several sites in the reporter gene (Figure 3). These observations suggest that the CpG methylation in the mammalian genome (Grünwald and Pfeifer, 1989) may contribute to the UVA1-induced mutation. The cytosine methylation in DNA is known to promote UVB/sunlight-induced CPD formation at cytosine-containing dipyrimidine sites (Drouin and Therrien, 1997; Tommasi *et al.*, 1997), and UVB, UVA2, and sunlight have been shown to induce C→T mutations frequently at those dipyrimidine sites associated with a methylated CpG (Pfeifer *et al.*, 2005; Ikehata and Ono, 2007). The results in this study might expand this concept of the effect of CpG methylation on UV genotoxicity from the UVB–UVA2 wavelength range to that of the UVA1. However, UVA1 did not induce mutations at the 5′-CCG-3′ sequence, which is the other triplet including both dipyrimidine and CpG motifs (Table 2). This discrepancy could be explained by the previous observation that UVA1 produced CPDs at 5′-TC-3′ and 5′-CT-3′ dipyrimidines but not at CC dipyrimidines in mammalian cellular and skin DNA, although the highest yield was observed at TT dipyrimidines (Courdavault *et al.*, 2004; Mouret *et al.*, 2006). If the photosensitization-mediated triplet energy transfer occurs specifically to thymines and produces CPDs selectively at thymine-containing dipyrimidines, and if cytosine methylation can promote this process, the preferential recovery of the UV-specific C→T mutation at the 5′-TCG-3′ would be explainable. Interestingly, the biased occurrence of the CpG-associated UV-specific mutation toward 5′-TCG-3′ against 5′-CCG-3′ is also noticed for the mutations in UVB-, sunlight-, and UVA2-exposed epidermis, which were reported in our previous studies (Ikehata *et al.*, 2003a, b, 2004), although the degrees of the bias are smaller than UVA1: numbers of the C→T mutation at 5′-TCG-3′ and 5′-CCG-3′ sites are 23 and 2 for UVB, 27 and 7 for sunlight, 49 and 4 for UVA2, and 70 and 4 for UVA1, respectively. In addition, most of the 5′-TCG-3′-associated C→T mutations detected in those previous studies occurred at the same specific hot spots as observed in this study, producing similar patterns of the hot spot distribution as that with UVA1 (Figure 3), although hot spots were less prominent in the UVB and sunlight patterns (Ikehata and Ono, 2007). This might

suggest that UV wavelengths shorter than UVA1 can also induce CPDs through the photosensitization-mediated triplet energy transfer mechanism, even though less efficient than UVA1. However, this presumption could not be accepted completely because the UV sources used in those studies also emit UVA1 as a part of their output (Ikehata *et al.*, 2004). Actually, the majority of the UV-specific C→T mutations detected in our UVB and sunlight studies did not occur at CpG sites (Table 1; Ikehata *et al.*, 2004), indicating that main pathways for the mutagenesis with those UV sources should be different from the CPD-mediated mechanism by UVA1 discussed above. A similar bias of C→T mutations toward 5′-TCG-3′ sites was also observed for the background mutation (10 mutations at 5′-TCG-3′ vs 5 mutations at 5′-CCG-3′). However, the extent of the bias was much smaller than any of those observed for the UV-induced mutations.

In this and previous studies (Ikehata *et al.*, 2003a), we demonstrated that UVA genotoxicity occurs mainly through CPD formation, not through ROS generation, in healthy skin. However, we should be cautious in using the results obtained from this study to predict genotoxic effects of UVA on human skin because human epidermis is much thicker than mouse epidermis, which might make a difference in responses of the dermal tissue to the UVA genotoxicity between humans and mice. Moreover, our studies indicate that, within the dose range of daily irradiance that we are exposed to under natural sunlight in the middle latitudes in midsummer, the skin genotoxicity by UVA1 is extremely small compared to that by UVB (Ikehata and Ono, 2002) or natural sunlight (Ikehata *et al.*, 2004): the UVA1 component in sunlight could induce MF in the epidermis only threefold at most above the background level even after a whole day of exposure on a clear day ($\leqslant 1\,MJ\,m^{-2}$), whereas the UVB component and total sunlight would cause increases of 15-fold and 35-fold, respectively, after just an hour of exposure at noon. Thus, the harmfulness of the UVA1 component of natural sunlight would appear to be negligible compared to the UVB and, probably, UVA2 components (Ikehata *et al.*, 2003a). However, we studied only the effect of a single exposure of UVA1. Repetitive irradiation might affect the situation. In fact, we showed previously that the delivery of multiple doses of UVB at a certain interval cancels the level-off suppression of the mutation induction observed in the epidermis and causes the reappearance of a dose-dependent MF increase (Ikehata and Ono, 2002). Accordingly, studies of UVA1 genotoxicity in this aspect should be conducted in the future.

MATERIALS AND METHODS

Mice and laser irradiation

All experimental procedures, including animal husbandry, were conducted according to the Guidelines for Animal Welfare and Experimentation at Tohoku University and the National Institutes of Natural Sciences. A transgenic mouse strain harboring λ-phage-based *lacZ* mutational reporter genes (Gossen *et al.*, 1989) was used. The UVA1 source used was a continuous-wave 364-nm Ar laser maintained by the National Institute for Basic Biology (Okazaki, Japan). The beam was expanded through a set of lenses to irradiate a 60×60 mm flat field at a homogeneous intensity of $300–400\,W\,m^{-2}$. Irradiation to the mouse skin was performed as described (Ikehata *et al.*, 2003a). Briefly, the depilated dorsal skin of anesthetized 8- to 12-week-old mice was irradiated in a black box and monitored with an infrared camera under lighting with 945-nm photodiodes. During the irradiation, no temperature increase was observed.

DNA damage assay

Mice exposed to 0, 0.85, 2, or $3\,MJ\,m^{-2}$ of the 364-nm laser light were killed immediately after irradiation, and the epidermal and dermal genomic DNA was isolated separately from the exposed skin area using a phenol–chloroform-based extraction method (performed at room temperature), and assayed for the quantification of CPD and 64PP as described (Ikehata *et al.*, 2007a) using mAbs specific to each photolesion, and analyzed for the quantification of 8-OH-dG using an HPLC equipped with an electrochemical detector as described (Kawai *et al.*, 2007). In the processes for 8-OH-dG quantification, DNA samples were stored at −80 °C at every step waiting for next treatments to avoid oxidation of the samples. For comparison of the efficiencies in the induction of the UV photolesions, UVB light was also irradiated with broadband UVB fluorescent lamps (peak emission 313 nm, FL20S.E; Toshiba, Tokyo, Japan).

Mutation analyses

Four weeks after irradiation, mice were killed. The epidermal and dermal genomic DNA isolated from the exposed skin was used for the detection of *lacZ* mutants, evaluation of the MFs, and analysis of the DNA sequence changes by the mutations (Wang *et al.*, 2006).

Statistical analyses

Differences in the dose-dependent induction kinetics of 8-OH-dG and UV photolesions were evaluated by two-way analysis of variance and a *post hoc* Bonferroni/Dunn's test. Irradiance (0, 0.85, 2, and $3\,MJ\,m^{-2}$) and tissue (epidermis and dermis) were set as the independent variables and the lesion amount as the dependent variable. For evaluation of the irradiance-dependent MF induction, linear regression analysis was performed under the presumption that the *y*-intercept equals the background MF. Differences between mutation spectra were estimated with the Adams–Skopek test (Cariello *et al.*, 1994) and Fisher's exact probability test.

CONFLICT OF INTEREST

The authors state no conflict of interest.

ACKNOWLEDGMENTS

We thank T Nakamura, M Suzuki, G Kawaguchi, M Kimura, A Yamamoto, N Yoshizaki, Y Hasegawa, A Miura, Y Ikeda, Y Takahashi, and Y Shono for experimental assistance, S Kikuchi for help with manuscript preparation, and B Bell for help in editing the manuscript. This study was carried out under the NIBB Cooperative Research Program for the Okazaki Large Spectrograph (4-507, 5-507, 6-511, and 7-509).

SUPPLEMENTARY MATERIAL

Table S1. *lacZ* mutations in 364-nm UVA1-exposed mouse skin epidermis.

REFERENCES

Agar NS, Halliday GM, StC Barnetson R, Ananthaswamy HN, Wheeler M, Jones AM (2004) The basal layer in human squamous tumors harbors more UVA than UVB fingerprint mutations: a role for UVA in human skin carcinogenesis. *Proc Natl Acad Sci USA* 101:4954–9

Besaratinia A, Kim S, Bates SE, Pfeifer GP (2007) Riboflavin activated by ultraviolet A1 irradiation induces oxidative DNA damage-mediated mutations inhibited by vitamin C. *Proc Natl Acad Sci USA* 104:5953–8

Besaratinia A, Synold TW, Chen H, Chang C, Xi B, Riggs AD *et al.* (2005) DNA lesions induced by UV A1 and B radiation in human cells: comparative analyses in the overall genome and in the *p53* tumor suppressor gene. *Proc Natl Acad Sci USA* 102:10058–63

Besaratinia A, Synold TW, Xi B, Pfeifer GP (2004) G-to-T transversions and small tandem base deletions are the hallmark of mutations induced by ultraviolet A radiation in mammalian cells. *Biochemistry* 43:8169–77

Bruls WAG, Slaper H, Van der Leun JC, Berrens L (1984) Transmission of human epidermis and stratum corneum as a function of thickness in the ultraviolet and visible wavelengths. *Photochem Photobiol* 40:485–94

Cariello NF, Piegorsch WW, Adams WT, Skopek TR (1994) Computer program for the analysis of mutational spectra: application to *p53* mutations. *Carcinogenesis* 15:2281–5

Courdavault S, Baudouin C, Charveron M, Favier A, Cadet J, Douki T (2004) Larger yield of cyclobutane dimers than 8-oxo-7,8-dihydroguanine in the DNA of UVA-irradiated human skin cells. *Mutat Res* 556:135–42

D'Errico M, Teson M, Calcagnile A, De Santis LP, Nikaido O, Botta E *et al.* (2003) Apoptosis and efficient repair of DNA damage protect human keratinocytes against UVB. *Cell Death Differ* 10:754–6

De Gruijl FR, Van der Leun JC (1994) Estimate of the wavelength dependency of ultraviolet carcinogenesis in humans and its relevance to the risk assessment of a stratospheric ozone depletion. *Health Phys* 67:319–25

De Laat A, Van der Leun JC, De Gruijl FR (1997) Carcinogenesis induced by UVA (365-nm) radiation: the dose-time dependence of tumor formation in hairless mice. *Carcinogenesis* 18:1013–20

Drobetsky EA, Turcotte J, Châteauneuf A (1995) A role for ultraviolet A in solar mutagenesis. *Proc Natl Acad Sci USA* 92:2350–4

Drouin R, Therrien J-P (1997) UVB-induced cyclobutane pyrimidine dimer frequency correlates with skin cancer mutational hot spots in *p53*. *Photochem Photobiol* 66:719–26

Friedberg EC, Walker GC, Siede W, Wood RD, Schultz RA, Ellenberger T (eds) (2005) *DNA repair and mutagenesis*. 2nd ed. Washington, DC: ASM Press

Gossen JA, De Leeuw WJF, Tan CHT, Zwarthoff EC, Berends F, Lohman PHM *et al.* (1989) Efficient rescue of integrated shuttle vectors from transgenic mice: a model for studying mutations *in vivo*. *Proc Natl Acad Sci USA* 86:7971–5

Grollman AP, Moriya M (1993) Mutagenesis by 8-oxoguanine: an enemy within. *Trends Genet* 9:246–9

Grünwald S, Pfeifer GP (1989) Enzymatic DNA methylation. *Prog Clin Biochem Med* 9:61–103

Ikehata H, Kudo H, Masuda T, Ono T (2003a) UVA induces C→T transitions at methyl CpG-associated dipyrimidine sites in mouse skin epidermis more frequently than UVB. *Mutagenesis* 18:511–9

Ikehata H, Masuda T, Sakata H, Ono T (2003b) Analysis of mutation spectra in UVB-exposed mouse skin epidermis and dermis: frequent occurrence of C→T transition at methylated CpG-associated dipyrimidine sites. *Environ Mol Mutagen* 41:280–92

Ikehata H, Nakamura S, Asamura T, Ono T (2004) Mutation spectrum in sunlight-exposed skin epidermis: small but appreciable contribution of oxidative stress-induced mutagenesis. *Mutat Res* 556:11–24

Ikehata H, Ono T (2002) Mutation induction with UVB in mouse skin epidermis is suppressed in acute high-dose exposure. *Mutat Res* 508:41–7

Ikehata H, Ono T (2007) Significance of CpG methylation for solar UV-induced mutagenesis and carcinogenesis in skin. *Photochem Photobiol* 83:196–204

Ikehata H, Saito Y, Yanase F, Mori T, Nikaido O, Ono T (2007a) Frequent recovery of triplet mutations in UVB-exposed skin epidermis of *Xpc*-knockout mice. *DNA Repair* 6:82–93

Ikehata H, Yanase F, Mori T, Nikaido O, Tanaka K, Ono T (2007b) Mutation spectrum in UVB-induced skin epidermis of *Xpa*-knockout mice: frequent recovery of triplet mutations. *Environ Mol Mutagen* 48:1–13

Kappes UP, Luo D, Potter M, Schulmeister K, Rünger TM (2006) Short- and long-wave UV light (UVB and UVA) induce similar mutations in human skin cells. *J Invest Dermatol* 126:667–75

Kawai K, Li Y, Kasai H (2007) Accurate measurement of 8-OH-dG and 8-OH-Gua in mouse DNA, urine and serum: effects of X-ray irradiation. *Genes Environ* 29:107–14

Kielbassa C, Epe B (2000) DNA damage induced by ultraviolet and visible light and its wavelength dependence. *Methods Enzymol* 319: 436–45

Klungland A, Rosewell I, Hollenbach S, Larsen E, Daly G, Epe B *et al.* (1999) Accumulation of premutagenic DNA lesions in mice defective in removal of oxidative base damage. *Proc Natl Acad Sci USA* 96:13300–5

Kvam E, Tyrrell RM (1997) Induction of oxidative DNA base damage in human skin cells by UV and near visible radiation. *Carcinogenesis* 18:2379–84

Lamola AA (1970) Triplet photosensitization and the photobiology of thymine dimers in DNA. *Pure Appl Chem* 24:599–610

Leccia MT, Richard MJ, Joanny-Crisci F, Beani JC (1998) UV-A1 cytotoxicity and antioxidant defence in keratinocytes and fibroblasts. *Eur J Dermatol* 8:478–82

Matsunaga T, Hieda K, Nikaido O (1991) Wavelength dependent formation of thymine dimers and (6-4)photoproducts in DNA by monochromatic ultraviolet light ranging from 150 to 365 nm. *Photochem Photobiol* 54:403–10

Mizuno T, Matsunaga T, Ihara M, Nikaido O (1991) Establishment of a monoclonal antibody recognizing cyclobutane-type thymine dimers in DNA: a comparative study with 64M-1 antibody specific for (6-4)photoproducts. *Mutat Res* 254:175–84

Mouret S, Baudouin C, Charveron M, Favier A, Cadet J, Douki T (2006) Cyclobutane pyrimidine dimers are predominant DNA lesions in whole human skin exposed to UVA radiation. *Proc Natl Acad Sci USA* 103: 13765–70

Orimo H, Tokura Y, Hino R, Kasai H (2006) Formation of 8-hydroxy-2′-deoxyguanosine in the DNA of cultured human keratinocytes by clinically used doses of narrowband and broadband ultraviolet B and psoralen plus ultraviolet A. *Cancer Sci* 97:99–105

Pfeifer GP, You Y, Besaratinia A (2005) Mutations induced by ultraviolet light. *Mutat Res* 571:19–31

Setlow RB, Grist E, Thompson K, Woodhead AD (1993) Wavelengths effective in induction of malignant melanoma. *Proc Natl Acad Sci USA* 90: 6666–70

Tessman I, Liu S-K, Kennedy MA (1992) Mechanism of SOS mutagenesis of UV-irradiated DNA: mostly error-free processing of deaminated cytosine. *Proc Natl Acad Sci USA* 89:1159–63

Tommasi S, Denissenko MF, Pfeifer GP (1997) Sunlight induces pyrimidine dimers preferentially at 5-methylcytosine bases. *Cancer Res* 57:4727–30

Tyrrell RM (2000) Role for singlet oxygen in biological effects of ultraviolet A radiation. *Methods Enzymol* 319:290–6

Van Kranen HJ, De Laat A, Van de Ven J, Wester PW, De Vries A, Berg RJW *et al.* (1997) Low incidence of *p53* mutations in UVA (365-nm)-induced skin tumors in hairless mice. *Cancer Res* 57:1238–40

Wang F, Saito Y, Shiomi T, Yamada S, Ono T, Ikehata H (2006) Mutation spectrum in UVB-exposed skin epidermis of a mildly-affected *Xpg*-deficient mouse. *Environ Mol Mutagen* 47:107–16

Wood SR, Berwick M, Ley RD, Walter RB, Setlow RB, Timmins GS (2006) UV causation of melanoma in *Xiphophorus* is dominated by melanin photosensitized oxidant production. *Proc Natl Acad Sci USA* 103: 4111–4115

Analytical Biochemistry 383 (2008) 236–242

Contents lists available at ScienceDirect

Analytical Biochemistry

journal homepage: www.elsevier.com/locate/yabio

Neopterin, a marker of immune response, and 8-hydroxy-2′-deoxyguanosine, a marker of oxidative stress, correlate at high age as determined by automated simultaneous high-performance liquid chromatography analysis of human urine

Peter Svoboda [a], Seong-Hee Ko [a,b], BeLong Cho [c], Sang-Ho Yoo [c], Seong-Won Choi [a], Sang-Kyu Ye [a], Hiroshi Kasai [d], Myung-Hee Chung [a,*]

[a] Department of Pharmacology, College of Medicine, Seoul National University, Seoul 110-799, South Korea
[b] Department of Food and Nutrition, College of Human Ecology, Sookmyung Women's University, Seoul 140-742, South Korea
[c] Department of Family Medicine, College of Medicine, Seoul National University, Seoul 110-799, South Korea
[d] Department of Environmental Oncology, Institute of Industrial Ecological Sciences, University of Occupational and Environmental Health, Kitakyushu 807-8555, Japan

ARTICLE INFO

Article history:
Received 15 June 2008
Available online 15 September 2008

Keywords:
8-Hydroxy-2′-deoxyguanosine
Neopterin
Oxidative stress
Immune response
Aging

ABSTRACT

Using an established high-performance liquid chromatography (HPLC) method based on anion exchange chromatography, fraction collection, and electrochemical detection, the oxidative DNA damage marker 8-hydroxy-2′-deoxyguanosine (8-OH-dG) can be analyzed rapidly and precisely in human urine samples. In addition, by ultraviolet (UV) detection, it was shown recently that it is possible to simultaneously analyze creatinine and 7-methylguanine (m^7Gua), an RNA degradation product, in urine. By adding a fluorescence detector to the HPLC system, we now report that it is also possible to detect pteridins such as neopterin and biopterin. The fluorescence detection was evaluated in detail for neopterin, an immune response and tumor marker. The urinary content of neopterin, assessed by using the HPLC method, was verified with a commercial neopterin enzyme-linked immunosorbent assay (ELISA) kit as indicated by the high correlation between the two methods ($r = 0.98$). In urinary samples from 58 young healthy individuals (male and female nonsmokers, ages 19–39 years), it was found that there was no significant correlation ($r = -0.04$) between the levels of 8-OH-dG and neopterin (as normalized to urinary creatinine levels). In contrast, in urinary samples from 60 old healthy individuals (male and female nonsmokers, ages 60–86 years), there was a significant correlation ($r = 0.47$) found between the levels of 8-OH-dG and neopterin (as normalized to urinary creatinine levels). These findings strongly indicate that the higher level of immune response that was correlating with old age contributes significantly to the higher level of oxidative damage as assessed in the form of 8-OH-dG. Using this type of HPLC system, it is possible to evaluate oxidative DNA damage and immune response simultaneously using the respective urinary markers. These data may contribute to understanding of the pathophysiology of diseases such as infections and tumor progression where both oxidative stress and immune response occur simultaneously.

A potentially mutagenic DNA base, 8-hydroxyguanine (8-OH-guanine or 8-oxo-guanine) is repaired, released from the cell, and eventually excreted via the urine as the base (8-OH-guanine) or the nucleoside, 8-hydroxy-2′-deoxyguanosine (8-OH-dG[1], 8-oxo-dG). The urinary content of 8-OH-dG represents an average rate of oxidative damage to guanine in the form of the free nucleotide (dGTP) and in DNA [1]. 8-OH-guanines in a mutational hot spot in fragments of the *c-Ha-ras* gene (an onco-gene activated in many human cancers) have a strong activating potential [2,3]. In vitro, such damage, through the action of DNA polymerases, has consequences such as misreplication, inhibition of replication, and mutagenesis described as "action at a distance" [2,3]. In vivo, increased levels of 8-OH-dG have been found in urine of various cancer patients [4].

A marker related to immune response is neopterin. It is formed when GTP cyclohydrolase 1 (GTPCH1) catalyzes the conversion of GTP to dihydroneopterin triphosphate, with further reactions leading to the formation of pteridins such as neopterin, biopterin, and tetrahydrobiopterin [5]. Neopterin levels are increased due to immune response activation. Gamma interferon produced from activated monocytes/macrophages produces high levels of neopterin

* Corresponding author. Fax: +82 2 745 7996.
E-mail address: mhchung@snu.ac.kr (M.-H. Chung).

[1] *Abbreviations used:* 8-OH-dG, 8-hydroxy-2′-deoxyguanosine; GTPCH1, GTP cyclohydrolase 1; HPLC, high-performance liquid chromatography; ECD, electrochemical detection; m^7Gua, 7-methylguanine; UV, ultraviolet; 8-OH-G, 8-hydroxyguanosine; EC, electrochemical; ELISA, enzyme-linked immunosorbent assay.

0003-2697/$ - see front matter © 2008 Elsevier Inc. All rights reserved.
doi:10.1016/j.ab.2008.09.014

and also oxygen free radicals due to the immune activation [5,6]. Thus, neopterin may be used as a marker for both immune system activation (e.g., viral infection) and oxidative stress [5,6]. Neopterin concentrations increase in patients with various malignant tumors, such as colon, ovarian, endometrial, cervical, renal, and breast cancer, as well as leukemia and lymphoma [7,8]. Also, in many cases, higher neopterin levels correlate with advance in tumor stage and severity in prognosis, and they decrease after successful therapy [7,8]. Also it has been shown that GTPCH1 may be inhibited by the oxidative stress markers 8-OH-GTP and 8-OH-dGTP [9]. Thus, increased oxidative stress could result in significant inhibition of GTPCH1 activity and aberrations in pteridin biosynthesis pathways. Defense systems against guanine oxidation, which protect cells against its mutagenic effects, may also protect against its inhibitory effects on metabolism via GTPCH1.

By using an automated high-performance liquid chromatography (HPLC) system and electrochemical detection (ECD), we showed previously that it is possible to analyze 8-OH-dG in human urine with high sensitivity and reproducibility. It was also shown that it is possible to simultaneously analyze the urinary content of creatinine and 7-methylguanine (m^7Gua) with an ultraviolet (UV) detector in the same sample run. The HPLC system is based on anion exchange chromatography in the first chromatography step, precise fraction collection of 8-OH-dG, and reversed-phase chromatography in the second chromatography step to detect 8-OH-dG electrochemically. Now we present a modification of this method that makes it possible to analyze the urinary content of neopterin, in addition to 8-OH-dG, in the same sample run. By using fluorescence detection, neopterin together with monapterin can be singled out as a peak separate from biopterin.

Although neopterin levels are known to increase with age, there is less known about the relationship between immune response (neopterin) and oxidative damage (8-OH-dG) as related to human aging. The purpose of this study was to confirm the accuracy of the new method to analyze 8-OH-dG and neopterin simultaneously and to look for age-related differences in the amount of these compounds in urine. Human urine samples from healthy donors were obtained and divided into two groups: urine from subjects of young age (19–39 years) and urine from subjects of old age (60–86 years).

Materials and methods

Materials

8-OH-dG, creatinine, m^7Gua, and d-(+)-neopterin, used to prepare standards, were obtained from Sigma-Aldrich (USA). D-Monapterin was obtained from Dr. Schirk's Laboratory (Switzerland). 8-Hydroxyguanosine (8-OH-G), used as a marker for fraction collection, was obtained from Cayman Chemical (USA). Biopterin was prepared from 7,8-dihydro-l-biopterin (Cayman Chemical).

Anion exchange resin MCI GEL CA08F (7 μm, Cl^- form) was purchased from Mitsubishi Chemical (Japan) and prepared as described previously [10] before being manually packed in a guard column (1.5 × 50 mm) and main column (1.5 × 150 mm) for use in the first chromatography step (HPLC-1). The column (Capcell Pak C18, 5 μm, 4.6 × 250 mm) used in the second chromatography step (HPLC-2), for analysis of the 8-OH-dG fraction, was purchased from Shiseido (Japan). Water, methanol, and acetonitrile of HPLC grade were purchased from Fisher Scientific (Korea).

HPLC analysis of 8-OH-dG, neopterin, and creatinine in human urine

Human urine samples were collected voluntarily during regular health checks of seemingly healthy subjects of Korean origin (male and female nonsmokers) at the Department of Family Medicine, Seoul National University College of Medicine (Korea). The samples were collected from 58 young subjects (31 men and 27 women, ages 19–39 years) and 60 old subjects (32 men and 28 women, ages 60–86 years). To minimize any interference due to various sampling times, urine samples were collected each morning at the same time (8–9 am). At the time for urine collection, the health of the subjects was evaluated using standard analytical procedures at the hospital clinical lab. From the samples assayed, the subjects to be included in this study were shown to be negative for diseases such as hypertension, diabetes, infection, and detectable cancers. In other words, their health was considered as normal. The urine samples to be analyzed for 8-OH-dG and neopterin were frozen at −20 °C for short time storage before being transferred to a −70 °C freezer.

Before analysis, urine samples were defrosted and mixed with an equal volume of a 4% acetonitrile solution containing the ribonucleoside marker 8-OH-G (120 μg/ml), 130 mM NaOAc, and 0.6 mM H_2SO_4. To remove any precipitates, the Eppendorf tubes containing the mixture were then stored at 6 °C in a refrigerator for 3 h before being centrifuged at 13,000 rpm for 5 min. Samples were transferred to plastic HPLC injector vials, and 20 μl was analyzed for 8-OH-dG by the use of an automated HPLC system similar to that described in detail previously [10].

In essence, the system was composed of a sampling injector (Gilson 231XL), a pump (Gilson 307) for the anion exchange guard and main column in HPLC-1 (the flow rate was 45 μl/min and the column oven was set at 65 °C), a UV detector (Gilson UV/VIS-151), a second pump (Gilson 307) and pulse damper (Gilson 805) for the analysis of the 8-OH-dG fraction with a reverse-phase column in HPLC-2 (the flow rate was 0.8 ml/min, and the column oven was set at 40 °C), connected with an electrochemical (EC) detector (ESA Coulochem II) and two switch valves (Gilson Valvemate). A third pump (Gilson 307) was used to back-wash the guard column (flow rate of 70 μl/min) for 32 min after valve switching at approximately 13 min after each sample injection. A scheme of the major instruments and conditions is presented in Fig. 1. The solvent used for HPLC-1 was 2% acetonitrile in 0.3 mM sulfuric acid, and the solvent for HPLC-2 was 10 mM phosphate buffer (pH 6.7) containing 5% methanol plus an antiseptic reagent MB (100 μl/ L). The solvents were recycled for a time period of 1 week. The guard column was back-washed with 0.5 M ammonium sulfate/acetonitrile (7:3, v/v). An online degasser was used to prevent formation of air bubbles. After the detection of creatinine at 245 nm [11], the wavelength was automatically switched to 305 nm to detect the 8-OH-G marker used for automatic peak detection [10,12]. The detection of 8-OH-G peak (controlled by software from Gilson) initialized a valve to collect the fraction containing 8-OH-dG. The 8-OH-dG fraction collected was subsequently injected onto HPLC-2 for detection of 8-OH-dG by an ESA Coulochem II EC detector with a guard cell (5020) and an analytical cell (5011) and the following applied potentials: guard cell = 410 mV, electrode 1 = 210 mV, and electrode 2 = 360 mV (Fig. 1). The total time between analyses of consecutive samples was 60 min.

For analysis of neopterin, a fluorescence detector (Soma S-3370, Japan) was connected in-line after the Gilson UV detector and the valve used for collection of 8-OH-dG fraction (Fig. 1). That way, the connections to the fluorescence detector did not interfere with the marker detection and fraction collection process. The fluorescence detector was set at excitation wavelength = 353 nm and emission wavelength = 438 nm. Because all samples were loaded at the beginning of the analysis, we used a Gilson 832 temperature regulator and thermostatic rack set to 4 °C (the actual measured temperature in the rack was 8 °C). That way, neopterin analysis was confirmed to be stable for up to at least 24 h. Also, samples were protected from any direct light source.

To verify the data of detection of urinary creatinine at 245 nm (see above), creatinine was also measured using a colorimetric

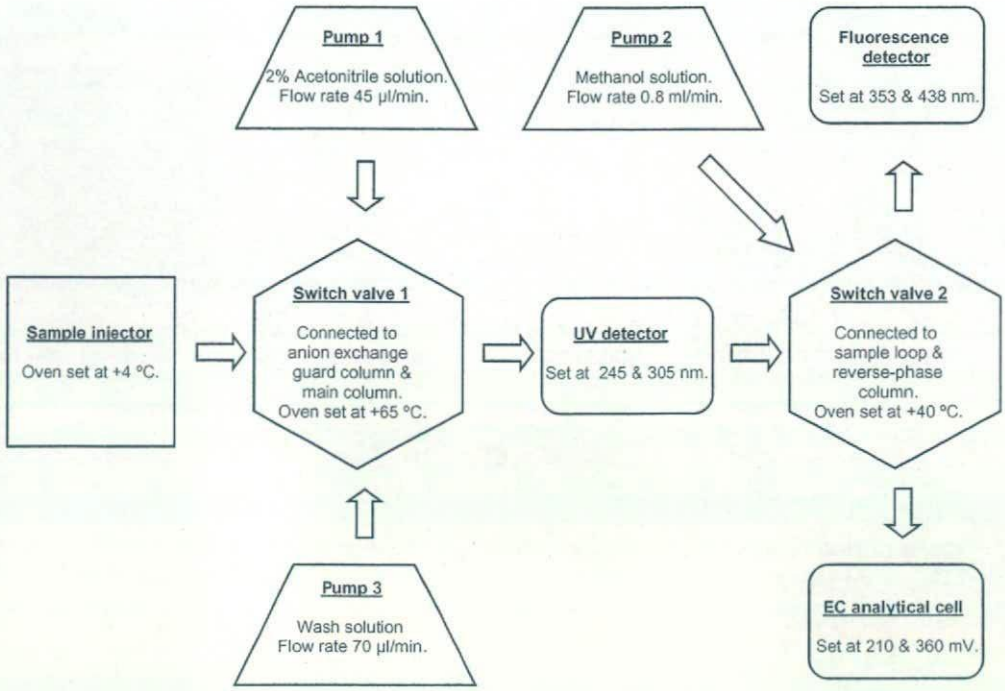

Fig. 1. Scheme of major instruments and conditions for the simultaneous analysis of urinary 8-OH-dG, neopterin, and creatinine.

method (hospital laboratory of Seoul National University, College of Medicine).

Verification of accuracy and stability of urinary neopterin HPLC analysis

To check stability of the neopterin analysis, samples were reinjected after 24 h at 8 °C. The peak position and any chance of adverse column matrix effects were tested by injecting urine samples spiked with pure neopterin. Four random urine samples were pooled, prepared as described above, and then spiked with known concentrations of a neopterin standard (0, 140, 280, and 420 ng/ml). For the spiked samples, the recovery of neopterin in HPLC-1 was calculated.

In addition, urine samples were spiked with fluorescent pteridins, monapterin and biopterin, to check elution positions relative to the elution position of neopterin. Neopterin and monapterin standards were prepared in diluted HCl. Biopterin was prepared from 7,8-dihydro-l-biopterin by iodide oxidation (1%) in 0.1 M NaOH for 60 min, and removal of iodide was done by adding ascorbate (1%). Finally, a commercial neopterin enzyme-linked immunosorbent assay (ELISA) kit (IBL, Germany) was used to confirm the HPLC yields. A subset of urine samples used in the HPLC analysis were diluted 10 times with deionized water and centrifuged at 13,000 rpm for 5 min. The supernatant was then diluted 10 times with the assay buffer found in the kit. The urine, which was diluted 100 times, underwent the reactions as specified in the manufacturer's instructions. Finally, the color density was measured at 450 nm with a photometer (kinetic microplate reader, Molecular Devices, USA). Final concentrations were calculated from the calibration curve based on the neopterin standard solutions included in the kit (0–111 nmol/L).

Calculation of results and statistics

The HPLC chromatograms were recorded with a Gilson 506C interface and integrated with computer software (Unipoint 3.30). Peaks were quantified by comparing the peak areas with those obtained from external standards analyzed on a daily basis. The external standard samples (5 ng 8-OH-dG/ml, 1 g creatinine/L, and 0.5 g neopterin/L) were prepared the same way as urine samples by mixing with an equal volume of a 4% acetonitrile solution containing the ribonucleoside marker (see above). Standard samples were injected separately from urine samples, and the mean value from at least three runs was used to calculate the peak area for the injected concentration. The concentration of a stock solution used to prepare the 8-OH-dG standard (before dilution to 5 ng/ml) was determined using a molar absorption extinction coefficient (ε) of 12,300 M^{-1} cm^{-1} at 245 nm in H_2O [12]. Similarly, the concentration of a stock solution of creatinine was determined using a molar absorption extinction coefficient (ε) of 7943 M^{-1} cm^{-1} at 235 nm in H_2O [13]. The concentration of the neopterin standard was checked with the commercial neopterin ELISA kit. The yields of 8-OH-dG and neopterin are presented after normalization to creatinine (µg/g creatinine).

To test for significant differences between the mean values in Table 2, the Student's t test was used. The correlation coefficients (r) and P values for the linear regressions presented in Figs. 3 and 4 were calculated using Microcal Origin software. The correlations were considered as significant at $P < 0.05$ based on analysis of variance and F test.

Results

Simultaneous analysis of 8-OH-dG and neopterin in human urine

Urine was spiked with standards of other fluorescent pterins to check elution positions. Neopterin, as detected by fluorescence detector, eluted at approximately 21 min, as seen by comparing the unspiked urine sample (Fig. 2A) with the neopterin-spiked urine (Fig. 2B). In Fig. 2A, the superimposed chromatogram (dotted line) shows the simultaneous UV detection of m^7Gua, creatinine, and 8-OH-G marker for peak detection, as has been described extensively before [10–12]. The chromatogram of urine spiked with monapterin shows that neopterin and monapterin elute at the same time (Fig. 2C). Thus, monapterin is expected to contribute

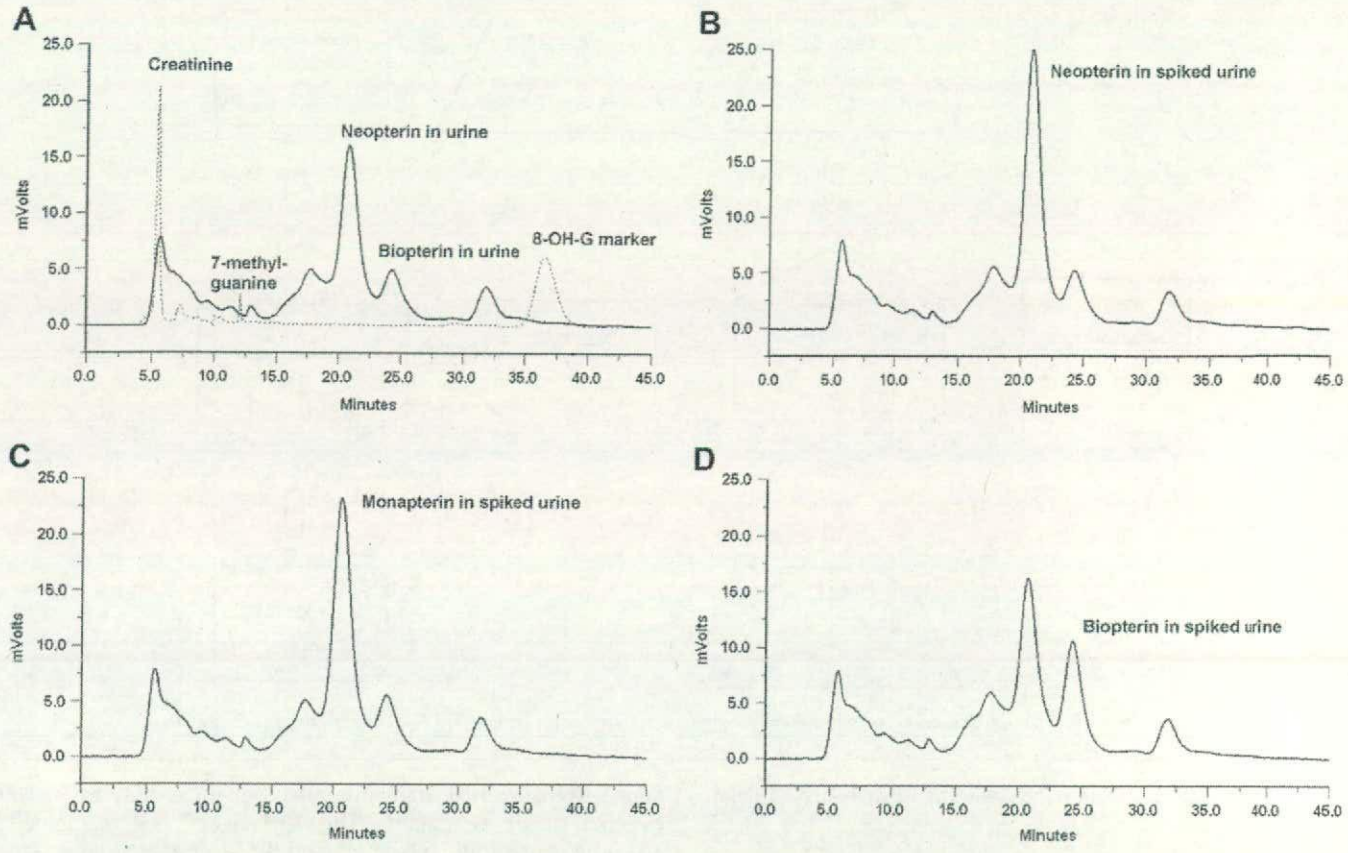

Fig. 2. Chromatograms of pooled urine from four humans. (A) Neopterin and biopterin in unspiked urine (total analyzed neopterin peak area corresponding to 549 ng/ml neopterin), UV detection of creatinine, m^7Gua, and 8-OH-G marker peaks are superimposed (dotted line). (B) Urine spiked with 420 ng/ml neopterin (total analyzed peak area corresponding to 949 ng/ml neopterin). (C) Urine spiked with 420 ng/ml monapterin (total analyzed peak area corresponding to 955 ng/ml neopterin). (D) Urine spiked with 420 ng/ml biopterin.

to the neopterin peak area of analyzed urine samples. Biopterin elutes at approximately 24 min, as seen by comparing the smaller peak seen in unspiked urine (Fig. 2A) with biopterin-spiked urine (Fig. 2D). Thus, it is evident that biopterin does not interfere with the neopterin peak area of analyzed urine samples. Although monapterin interferes with the neopterin peak, it contributes to only approximately 10% of the total peak area in urine samples, as has been shown previously [14].

Evaluation of neopterin stability and recovery from spiked human urine

To check the stability of the neopterin analysis, 18 randomly selected samples were reinjected after 24 h at 8 °C. The results showed that the area corresponding with the neopterin peak increased by 4.4 ± 2.8% (mean value ± standard deviation) (data are not shown). The small increase over time may be attributed to low-level oxidation of nonfluorescent dihydroneopterin to fluorescent neopterin. For this reason, the injections of samples were done within 12 h. Thus, it is expected that the error in the amount of neopterin detected in urine samples, as presented in tables and figures, would never be larger than approximately 2%.

Pooled urine samples were spiked with neopterin standard to 0, 140, 280, and 420 ng/ml (Table 1). All spiked samples had neopterin recoveries close to 100% and showed a linear increase in the amount of neopterin detected (Table 1). This would mean that the detected neopterin peak was not affected by any coprecipitation with urine components prior to analysis or by any urine sample matrix effects during chromatography. As an example, when a urine sample containing 549 ng/ml neopterin was spiked with 420 ng/ml neopterin standard, we obtained a peak area equivalent to 949 ng/ml neopterin (cf. Fig. 2A with Fig. 2B).

Table 1
Recovery of neopterin from spiked urine of humans

Added neopterin (ng/ml)	Urine from humans[a]	
	Detected neopterin[b] (ng/ml)	Recovery neopterin[b] (%)
0	556 ± 24	
140	703 ± 28	105 ± 7
280	858 ± 28	108 ± 7
420	1009 ± 20	108 ± 9

[a] Each value is based on four repeated analyses of pooled urine samples from humans ($n = 4$). The linear correlation between added and detected neopterin in human urine is $r = 0.98$.
[b] Mean values ± standard deviations are presented.

Correlation in detection of urinary neopterin levels between the HPLC method and a commercial ELISA kit

For the data from 20 human nonsmokers, the linear relationship (Y = slope x X – intercept) between the ELISA and HPLC methods for the concentrations [ng/ml] of urinary neopterin (including monapterin) is [neopterin concentration as determined by HPLC] = 1.02 x [neopterin concentration as determined by ELISA] – 57 (see the correlation line in Fig. 3), with an excellent correlation coefficient (r) equal to 0.98. To check for any discrepancy in the linear relationship due to age groups, these data were also recalculated for young and old subjects separately. Thus, for the old subjects (8 subjects ages 61–81 years), the linear relationship

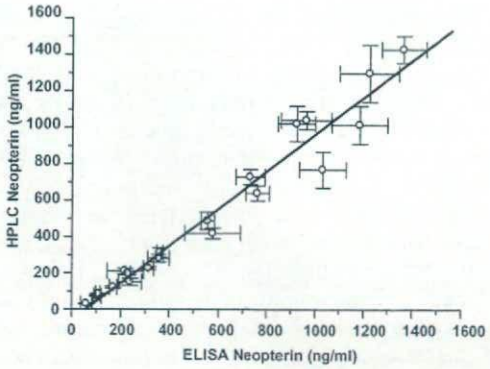

Fig. 3. Regression line for the correlation ($r = 0.98$) between urinary neopterin (including monapterin) levels as analyzed by HPLC with fluorescence detection and those obtained by a commercial neopterin ELISA kit. Urinary samples were measured from $n = 20$ individuals. Each data point represents the mean value and standard deviation from three independent experiments.

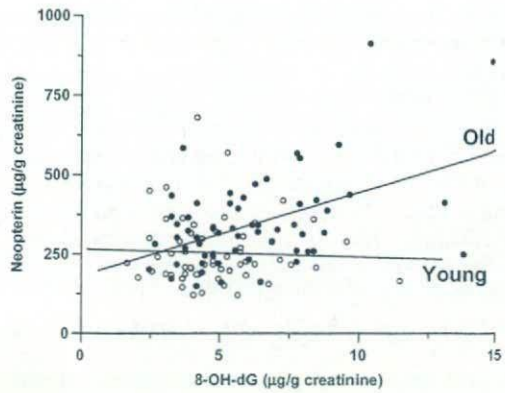

Fig. 4. Regression lines for correlations between human urinary 8-OH-dG and neopterin (including monapterin) content. ○, Regression line for the correlation ($r = -0.04$) between human urinary 8-OH-dG and neopterin content ($n = 58$ individuals, ages 19–39 years). ●, Regression line for the correlation ($r = 0.47$) between human urinary 8-OH-dG and neopterin content ($n = 60$ individuals, ages 60–86 years).

Table 2
Urinary excretion of 8-OH-dG and neopterin

	8-OH-dG[a] (µg/g creatinine)[b]	Neopterin[a] (µg/g creatinine)[c]
Young healthy subjects ($n = 58$, ages 19–39 years)	4.9 ± 1.9	254 ± 106
	(5.0 ± 1.7)	(260 ± 125)
Old healthy subjects ($n = 60$, ages 60–86 years)	6.2 ± 2.6	345 ± 145
	(6.0 ± 2.4)	(336 ± 134)

[a] Mean values ± standard deviations are presented for 8-OH-dG and neopterin normalized to creatinine values as detected at 245 nm and as detected by a colorimetric method for verification (in parentheses).

[b] Mean values of 8-OH-dG as normalized to creatinine are significantly different between young and old healthy subjects ($P < 0.01$).

[c] Mean values of neopterin as normalized to creatinine are significantly different between young and old healthy subjects ($P < 0.001$).

is [neopterin concentration as determined by HPLC] = 1.11 *x* [neopterin concentration as determined by ELISA] − 104, with *r* equal to 0.99 (correlation line not shown in Fig. 3). For the young subjects (12 subjects ages 21–38 years), the linear relationship is [neopterin concentration as determined by HPLC] = 0.91 *x* [neopterin concentration as determined by ELISA] − 13, with *r* equal to 0.97 (correlation line not shown in the figure).

8-OH-dG levels as compared with neopterin levels in human urine from healthy individuals

Urine samples collected were divided into two groups according to the ages of urine donors: samples from young subjects (ages 19–39 years) and samples from old subjects (ages 60–86 years). After normalization of urinary 8-OH-dG levels with urinary creatinine levels (µg/g creatinine), we found that the old subjects' urine had significantly higher levels (27% higher) of 8-OH-dG (6.2 µg/g creatinine) as compared with young subjects' urine (4.9 µg/g creatinine) (Table 2). In young subjects, female levels of 8-OH-dG (5.0 µg/g creatinine) were 1% higher than male levels (4.9 µg/g creatinine); in old subjects, female levels (6.3 µg/g creatinine) were 2% higher than male levels (6.1 µg/g creatinine).

For neopterin, old subjects' levels (345 µg/g creatinine) were significantly higher (36% higher) than young subjects' levels (254 µg/g creatinine) (Table 2). In young subjects, female levels of neopterin (312 µg/g creatinine) were 53% higher than male levels (204 µg/g creatinine); in old subjects, female levels (383 µg/g creatinine) were 23% higher than male levels (312 µg/g creatinine).

Interestingly, there was a significant correlation ($P < 0.001$) between the levels of 8-OH-dG and neopterin in old subjects' urine (Fig. 4). In old subjects' urine, the neopterin content increased with the increase of 8-OH-dG content, the correlation coefficient was $r = 0.47$ ($r^2 = 0.23$), and the slope was +26 (Fig. 4). Dividing the old subjects' data into two age groups, those between 60 and 64 years (16 men and 16 women) and those between 65 and 86 years (16 men and 12 women) yielded a similar trend, giving the correlation coefficients of $r = 0.57$ and 0.39 with slopes of +40 and +18, respectively (correlation lines not shown in Fig. 4). In young subjects' urine, however, there was no significant correlation between neopterin and 8-OH-dG levels, the correlation coefficient was $r = -0.04$, and the slope was −2 (Fig. 4).

Discussion

Simultaneous analysis of markers of oxidative stress and immune activation

We have shown that it is possible to analyze an oxidative damage marker (8-OH-dG) and an immune response marker (neopterin) simultaneously in the same analysis run using an HPLC method based on fluorescence and electrochemical detection. The uses of automated sample injection, fraction collection, and column switching make it possible to process a large number of urine samples with a high degree of analysis accuracy. Previously, we used this system to analyze 8-OH-dG rapidly and reliably in urine of humans, rats, mice, and other species [10–12,15]. The 8-OH-dG content in urine can be considered as a reliable indicator of whole-body oxidation processes, not obscured by artifactual oxidation of deoxyguanosine, such as could be the case during extraction of DNA from cellular samples.

By attaching a fluorescence detector to the previously described HPLC system [10–12,15], it is also possible to detect neopterin in human urine. Neopterin is separated in the first chromatography step using a column filled with anion exchange resin (see Materials and Methods). Furthermore, neopterin (Figs. 2A and 2B) was clearly separated from biopterin (Fig. 2D). However, it was not possible to resolve monapterin from the neopterin (cf. Fig. 2B with Fig. 2C). Monapterin has fluorescence activity similar to that of neopterin but constitutes only a minor level (~ 10%) of the total neopterin peak detected [14,16]. The relative amounts of monapterin to neopterin are expected to be fairly constant between individuals as well as between healthy subjects and patients with

diseases [14,17]. Urinary neopterin levels were kept constant by keeping the samples cool using a thermostatic rack during automatic sample injections on the HPLC device (see Materials and Methods). The small increase (+2%) in neopterin peak area of analyzed urine (see "Evaluation of Neopterin Stability and Recovery from Spiked Human Urine" subsection above) was likely due to oxidation of dihydroneopterin, reported to be approximately three times more abundant in human urine than neopterin [5,17]. Thus, it may be concluded that the peak analyzed as "neopterin" in our analysis (see Materials and Methods) constitutes approximately 90% of neopterin and 10% of monapterin.

Comparison of the levels of neopterin detected with our HPLC method with those obtained from a commercial neopterin ELISA kit (Fig. 3) revealed a very good correlation between the two methods ($r = 0.98$) and a slope of 1.02 (Fig. 3). Even though the neopterin data from the HPLC method included 10% monapterin, the values were not higher as compared with the ELISA method. This could be explained by some cross-reactivity in the ELISA with other components in the urine such as the other forms of pterins. As stated in the manufacturer's (IBL) instruction sheet, there is a cross-reactivity for dihydroneopterin of 3.5% and for monapterin of 0.3%. Because the level of dihydroneopterin is expected to be up to three times higher than the level of neopterin in human urine [5,17], dihydroneopterin alone could account for approximately 10% of the detected neopterin level in the ELISA. For this reason, the neopterin values from the HPLC detection and IBL ELISA were compared without any correction for the possible inclusion of the other pteridins (Fig. 3). Our values for urinary neopterin (men and women combined), when recalculated from micrograms/gram creatinine (Table 2) to micromoles/mole creatinine, are 114 μmol/mol creatinine in young subjects (ages 19–39 years) and 154 μmol/mol creatinine in old subjects (ages 60–86 years). These values correlate well with the means (men and women combined) of published reference values: 113 μmol/mol creatinine (ages 26–35 years) and 142 μmol/mol creatinine (age > 65 years) [5]. These comparisons, as well as the similar linear relationships between our HPLC method and an ELISA kit for both young and old subjects' neopterin levels (see "Correlation in Detection of Urinary Neopterin Levels between the HPLC Method and a Commercial ELISA Kit" subsection above), indicate that the monapterin/neopterin ratio does not change detectably during aging. In addition, it has been reported that the monapterin/neopterin ratio does not change due to various cancers [14].

In conclusion, even though our method for neopterin detection included monapterin, the accuracy of urinary neopterin determination for young and old subjects is directly comparable between the two assays (HPLC vs. IBL ELISA).

Oxidative damage as related to aging

Previously, we have shown the excreted urinary level of 8-OH-dG to be 4.2 μg/g creatinine in healthy male individuals (ages 18–58 years) [12,18]. In Table 2, a value of 4.9 μg/g creatinine is presented for the urinary content of 8-OH-dG in a group of healthy male and female individuals (ages 19–39 years). The somewhat higher value (4.9 vs. 4.2 in the previous study) may be explained by a different location, age distribution, and sex distribution of the subjects. Regarding the sex of the subjects, it has only little importance given that the urinary levels of 8-OH-dG are not higher than 2% in females as compared with males in our new study (see Results).

In old subjects' urine, the level of 8-OH-dG was 27% higher than that in young subjects (Table 2). This means that at old age (60–86 years), levels of 8-OH-dG excreted into urine increased significantly (Table 2). According to data from the literature, in the range between 35 and 65 years, age was not related to urinary 8-OH-dG excretion [19]. Also, based on a multiregression analysis, we showed previously that, among other factors, age (18–58 years) had a significant reducing effect on the urinary 8-OH-dG levels [18]. However, in the mentioned references [18,19], the maximum age of examined subjects was 65 years; thus, those data are not directly comparable with our new data presented in Table 2, based on subjects ages 60 to 86 years. In another published study [20], the levels of 8-OH-dG in old ($\geqslant$ 70 years) nonsmokers' urine were increased 136% over those found in young (< 40 years) subjects' urine. Although both our results (Table 2) and those presented in the mentioned study [20] show an increase of urinary 8-OH-dG at old age, the levels are much higher in the mentioned study. The method used to detect 8-OH-dG in that study [20] was based on an immunoassay (8-OH-dG Check ELISA kit) that may be prone to cross-reactivity with other urinary components, possibly explaining the higher values found. This immunoassay has been shown to correlate well with an HPLC–ECD analysis, although the former method showed two times higher values than the HPLC–ECD method [21,22]. In addition, a fraction of the samples analyzed by ELISA showed more than fourfold higher levels of 8-OH-dG [22]. Thus, for more exact determination of urinary 8-OH-dG concentrations, the HPLC–ECD method is preferred.

In Table 2, the data for 8-OH-dG excretion (as normalized to urinary creatinine levels) are presented without any corrections due to a possible age-dependent change in creatinine excretion. Because of a decreased glomerular filtration rate during aging, the urinary creatinine content will be lower in old persons as compared with young persons [23]. However, this should not change the ratio between 8-OH-dG and creatinine excreted given that the decreased glomerular filtration would also decrease the 8-OH-dG urinary content by a similar amount. As an example, creatinine clearance in old women (> 70 years) decreased 43% as compared with young women (< 40 years) [23]. However, this decrease was accompanied by a 42% lower excretion of creatinine in the old women [23]. Because plasma creatinine levels remain at a similar level during aging, the concurrent decrease in creatinine clearance and excretion may be explained by a reduction in lean body mass [23], with less muscle tissue producing less creatinine. Regarding 8-OH-dG excretion, it was suggested previously that it should be corrected for lean body mass because lean persons may have a higher metabolic rate and, thus, produce more 8-OH-dG [24]. Similarly, when lean body mass decreases during aging, a concurrent decrease in 8-OH-dG excretion would be expected.

In conclusion, our new data (Table 2) indicate that an increased urinary output of 8-OH-dG due to aging is not evident until subjects reach a more advanced age of at least 60 years.

Relation between immune activation and oxidative damage at old age

Human neopterin levels have been shown to increase during aging [5,25]. We found a 36% increase of urinary neopterin in old subjects as compared with young subjects (Table 2). In healthy old persons, it has been speculated that this could be attributed to immune activation due to the progression of age-related diseases, such as atherosclerosis and neurodegenerative disorders, although not yet clinically detectable [5,25]. It has been shown that diseases such as atherosclerosis, Alzheimer's dementia, Huntington's disease, as well as various types of malignancies and autoimmune diseases, are correlated with increased neopterin levels [8,26–29].

In healthy young subjects (19–39 years), we could not detect any correlation between urinary levels of neopterin and 8-OH-dG (Fig. 4). Because there is no evident immune response taking place in the healthy young group, there would be a normal level of oxygen radical production expected and the levels of 8-OH-dG would be dependent on individual factors such as individual repair capac-

ity for this lesion. Interestingly, in the healthy old subjects' (60–86 years) urine, however, there was an evident correlation found between neopterin and 8-OH-dG (Fig. 4). Increased immune activation as detected by increased neopterin levels, due to the activation of monocytes/macrophages, is followed by an increase in the levels of hydrogen peroxide and reactive oxygen species [5,6]. Therefore, it would be expected that the higher levels of neopterin in the old subjects' urine should correlate with increased formation of the oxidative damage marker 8-OH-dG, as seen in Fig. 4. Evidently, immune system activation, due to clinically undetected disease processes in persons of old age, contribute significantly to the higher level of oxidative damage in the form of 8-OH-dG, as found in excreted urine.

Conclusion

A new method based on HPLC with fluorescence and electrochemical detection was developed to analyze markers of immune response (neopterin) and oxidative damage (8-OH-dG) simultaneously in human urine. Neopterin levels detected were verified using standards of various forms of pteridins and by comparison with a neopterin immunoassay kit. The detected levels of neopterin and 8-OH-dG in urine correlate well with previous data. The method also shows promise of detection of another pterin, biopterin, although its detection was not verified in this report. Regarding the oxidative damage marker 8-OH-dG, it was shown to be excreted in higher levels in urine of subjects of old age (> 60 years). At old age, it was seen that increased levels of neopterin in urine correlated with increased levels of the oxidative damage marker 8-OH-dG. We conclude that immune system activation, possibly due to clinically undetected disease processes taking place in healthy old persons, contributes significantly to the level of oxidative damage in the form of 8-OH-dG.

Acknowledgments

This work was supported by a grant (2006-02293) from the Korea Science and Engineering Foundation (KOSEF) and the 2005 Brain Pool Program of the Korean Federation of Science and Technology Societies.

References

[1] S. Loft, H.E. Poulsen, Markers of oxidative damage to DNA: Antioxidants and molecular damage, Methods Enzymol. 300 (1999) 166–184.
[2] P. Jaloszynski, C. Masutani, F. Hanaoka, A.B. Perez, S. Nishimura, 8-Hydroxyguanine in a mutational hotspot of the *c-Ha-ras* gene causes misreplication, "action-at-a-distance" mutagenesis, and inhibition of replication, Nucleic Acids Res. 31 (2003) 6085–6095.
[3] P. Jaloszynski, E. Ohashi, H. Ohmori, S. Nishimura, Error-prone and inefficient replication across 8-hydroxyguanine (8-oxoguanine) in human and mouse ras gene fragments by DNA polymerase kappa, Genes Cells 10 (2005) 543–550.
[4] C. Tagesson, M. Kallberg, C. Klintenberg, H. Starkhammar, Determination of urinary 8-hydroxydeoxyguanosine by automated coupled-column high performance liquid chromatography: A powerful technique for assaying in vivo oxidative DNA damage in cancer patients, Eur. J. Cancer A 31 (1995) 934–940.
[5] C. Murr, B. Widner, B. Wirleitner, D. Fuchs, Neopterin as a marker for immune system activation, Curr. Drug Metab. 3 (2002) 175–187.
[6] C. Murr, L.C. Fuith, B. Widner, B. Wirleitner, G. Baier-Bitterlich, D. Fuchs, Increased neopterin concentrations in patients with cancer: Indicator of oxidative stress?, Anticancer Res 19 (1999) 1721–1728.
[7] B. Melichar, D. Solichova, R.S. Freedman, Neopterin as an indicator of immune activation and prognosis in patients with gynecological malignancies, Intl. J. Gynecol. Cancer 16 (2006) 240–252.
[8] A. Berdowska, K. Zwirska-Korczala, Neopterin measurement in clinical diagnosis, J. Clin. Pharm. Ther. 26 (2001) 319–329.
[9] Y. Tanaka, N. Nakagawa, S. Kuramitsu, S. Yokoyama, R. Masui, Novel reaction mechanism of GTP cyclohydrolase: I. High-resolution X-ray crystallography of *Thermus thermophilus* HB8 enzyme complexed with a transition state analogue, the 8-oxoguanine derivative, J. Biochem. (Tokyo) 138 (2005) 263–275.
[10] H. Kasai, A new automated method to analyze urinary 8-hydroxydeoxyguanosine by a high-performance liquid chromatography–electrochemical detector system, J. Radiat. Res. 44 (2003) 185–189.
[11] H. Kasai, P. Svoboda, S. Yamasaki, K. Kawai, Simultaneous determination of 8-hydroxydeoxyguanosine, a marker of oxidative stress, and creatinine, a standardization compound, in urine, Industr. Health 43 (2005) 333–336.
[12] P. Svoboda, H. Kasai, Simultaneous HPLC analysis of 8-hydroxydeoxyguanosine and 7-methylguanine in urine from humans and rodents, Anal. Biochem. 334 (2004) 239–250.
[13] R.C. Weast, CRC Handbook of Chemistry and Physics, CRC Press, Boca Raton, FL, 1978.
[14] S. Ogiwara, T. Nagatsu, R. Teradaira, K. Fujita, T. Sugimoto, Diastereomers of neopterin and biopterin in human urine, Biol. Chem. Hoppe Seyler 373 (1992) 1061–1065.
[15] P. Svoboda, M. Maekawa, K. Kawai, T. Tominaga, K. Savela, H. Kasai, Urinary 8-hydroxyguanine may be a better marker of oxidative stress than 8-hydroxydeoxyguanosine in relation to the life spans of various species, Antioxid. Redox Signal. 8 (2006) 985–992.
[16] C. Ahn, J. Byun, J. Yim, Purification, cloning, and functional expression of dihydroneopterin triphosphate 2-epimerase from *Escherichia coli*, J. Biol. Chem. 272 (1997) 15323–15328.
[17] O. Fuchs, S. Miistlen, A. Kramer, G. Reibnegger, E.R. Werner, J.J. Goedert, S. Kaufman, H. Wachter, Urinary neopterin concentrations vs. total neopterins for clinical utility, Clin. Chem. 35 (1989) 2305–2307.
[18] H. Kasai, N. Iwamoto-Tanaka, T. Miyamoto, K. Kawanami, S. Kawanami, R. Kido, M. Ikeda, Lifestyle and urinary 8-hydroxydeoxyguanosine, a marker of oxidative DNA damage: Effects of exercise, working conditions, meat intake, body mass index, and smoking, Jpn. J. Cancer Res. 92 (2001) 9–15.
[19] H.E. Poulsen, S. Loft, H. Prieme, K. Vistisen, J. Lykkesfeldt, K. Nyyssonen, J.T. Salonen, Oxidative DNA damage in vivo: Relationship to age, plasma antioxidants, drug metabolism, glutathione-S-transferase activity, and urinary creatinine excretion, Free Radic. Res. 29 (1998) 565–571.
[20] Y. Mizushima, S. Kan, S. Yoshida, S. Sasaki, S. Aoyama, T. Nishida, Changes in urinary levels of 8-hydroxy-2-deoxyguanosine due to aging and smoking, Geriatr. Gerontol. Intl. 1 (2001) 52–55.
[21] R. Yoshida, Y. Ogawa, H. Kasai, Urinary 8-oxo-7, 8-dihydro-2-deoxyguanosine values measured by an ELISA correlated well with measurements by high-performance liquid chromatography with electrochemical detection, Cancer Epidemiol. Biomarkers Prev. 11 (2002) 1076–1081.
[22] K. Shimoi, H. Kasai, N. Yokota, S. Toyokuni, N. Kinae, Comparison between high-performance liquid chromatography and enzyme-linked immunosorbent assay for the determination of 8-hydroxy-2-deoxyguanosine in human urine, Cancer Epidemiol. Biomarkers Prev. 11 (2002) 767–770.
[23] W. Musch, L. Verfaillie, G. Decaux, Age-related increase in plasma urea level and decrease in fractional urea excretion: Clinical application in the syndrome of inappropriate secretion of antidiuretic hormone, Clin. J. Am. Soc. Nephrol. 1 (2006) 909–914.
[24] S. Loft, K. Vistisen, M. Ewertz, A. Tjønneland, K. Overvad, H.E. Poulsen, Oxidative DNA damage estimated by 8-hydroxydeoxyguanosine excretion in humans: Influence of smoking, gender, and body mass index, Carcinogenesis 13 (1992) 2241–2247.
[25] H. Schennach, C. Murr, E. Gächter, P. Mayersbach, D. Schönitzer, D. Fuchs, Factors influencing serum neopterin concentrations in a population of blood donors, Clin. Chem. 48 (2002) 643–645.
[26] G. Weiss, J. Willeit, S. Kiechl, D. Fuchs, E. Jarosch, F. Oberhollenzer, G. Reibnegger, G.P. Tilz, F. Gerstenbrand, H. Wachter, Increased concentrations of neopterin in carotid atherosclerosis, Atherosclerosis 106 (1994) 263–271.
[27] E.P. Gurfinkel, B.M. Scirica, G. Bozovich, A. Macchia, E. Manos, B. Mautner, Serum neopterin levels and the angiographic extent of coronary arterial narrowing in unstable angina pectoris and in non-Q-wave acute myocardial infarction, Am. J. Cardiol. 83 (1999) 515–518.
[28] F. Leblhuber, J. Walli, K. Jellinger, G.P. Tilz, B. Widner, F. Laccone, D. Fuchs, Activated immune system in patients with Huntington's disease, Clin. Chem. Lab. Med. 36 (1998) 747–750.
[29] F. Leblhuber, J. Walli, U. Demel, G.P. Tilz, B. Widner, D. Fuchs, Increased serum neopterin concentrations in patients with Alzheimer's disease, Clin. Chem. Lab. Med. 37 (1999) 429–431.

J Occup Health 2008; 50: 366–372

Journal of Occupational Health

Field Study

The Stability of the Oxidative Stress Marker, Urinary 8-hydroxy-2'- deoxyguanosine (8-OHdG), when Stored at Room Temperature

Yuki MATSUMOTO[1], Yasutaka OGAWA[1], Rie YOSHIDA[1], Ayako SHIMAMORI[2], Hiroshi KASAI[3] and Hisayoshi OHTA[4]

[1]National Institute of Occupational Safety and Health, [2]School of Allied Health Sciences, Kitasato University, [3]Department of Environmental Oncology, University of Occupational and Environmental Health, Japan and [4]Graduate School of Medical Science, Kitasato University, Japan

Abstract: The Stability of the Oxidative Stress Marker, Urinary 8-hydroxy-2'- deoxyguanosine (8-OHdG), when Stored at Room Temperature: Yuki MATSUMOTO, *et al.* National Institute of Occupational Safety and Health—We examined the stabilities of urinary 8-hydroxy-2'-deoxyguanosine (8-OHdG) stored at room temperature (25°C) for 24 h or at –80°C for 800 days. Subjects were 19 males and 17 females aged 23–58 yr for the 24-h study, and 9 males and 4 females aged 24–54 yr for the 800-day study. We obtained information on the subjects by questionnaires and interviews. The level of urinary 8-OHdG was measured by HPLC using two-step separations. There were no significant changes of amount of urinary 8-OHdG under either storage conditions. We conclude that urine samples can be stored at 25°C and below for 24 h, when the research purpose includes the determination of urinary 8-OHdG. Urinary 8-OHdG was also stable for over two years when stored at –80°C. *(J Occup Health 2008; 50: 366–372)*

Key words: Oxidative stress, 8-hydroxy-2'-deoxyguanosine, Urine, HPLC-ECD

Urinary 8-hydroxy-2'-deoxyguanosine (8-OHdG), which is an oxidatively damaged nucleoside and may be a repair product of DNA or the nucleotide pool[1], has been widely used as a marker for evaluating *in vivo* oxidative stress[2, 3]. It has also been widely used as a health effect marker for workers who have been exposed to chemicals[4–9]. Urinary 8-OHdG is stable when stored at 4°C for 19 days[10], and also after 6 years of storage at –20°C[11], but to our knowledge there is no report about its stability at room temperature, that is 25°C. If a researcher wants to measure a 24-hours (24-h) period urinary excretion of 8-OHdG, he has to cool or freeze the urine samples immediately after each collection. However, it is not easy to do so unless the study is carried out at a place where the researcher can easily access refrigerators or freezers. If it is not necessary to store samples under special cooling conditions, urine collection will be more affordable.

This study aimed to evaluate the stability of urinary 8-OHdG kept at room temperature for a 24-h period (24-h room temperature study) and at –80°C for 800 days (800-d freezing study).

Subjects

Sample size

First we calculated the sample size that would satisfy our purpose[12]. To test whether the population mean μ is larger than μ_0 using the one-sided test, when the population variance is unknown, the least necessary sample size will be

$$n \approx \left(\frac{Z_\alpha - Z_{1-\beta}}{\Delta_0}\right)^2 + \frac{Z_\alpha^2}{2}$$

Δ_0 was defined by the formula $|\mu-\mu_0|/\sigma \geq \Delta_0$, which is the minimum normalized difference needed to reject the null hypothesis at a significance level of α with a power $1-\beta$. Using the detection limit and SD of our laboratory, we obtained $|\mu-\mu_0|=1.0$ and $\sigma=1.3$, and as a result $\Delta_0=|1.0|/1.3=0.77$. If we use $1-\beta=0.80$ and $\alpha=0.05$ for the test condition, the appropriate sample size is calculated as $n \geq 13$.

Subjects

All subjects were informed of the purpose and the

Received Oct 31, 2007; Accepted Apr 8, 2008
Published online in J-STAGE Jun 18, 2008
Correspondence to: Y. Ogawa, National Institute of Occupational Safety and Health, 6–21–1 Nagao, Tama-ku, Kawasaki 214-8585, Japan (e-mail: ogawa@h.jniosh.go.jp)